This papers appears in Mechatronics.
https://doi.org/10.1016/j.mechatronics.2019.102255

A cooperative paradigm for task-space control of multilateral nonlinear teleoperation with bounded inputs and time-varying delays

Amir Zakerimanesh[a], Farzad Hashemzadeh[a,*], Ali Torabi[b], Mahdi Tavakoli[b]

[a]Faculty of Electrical and Computer Engineering, University of Tabriz, Tabriz, Iran
[b]Department of Electrical and Computer Engineering, University of Alberta, Edmonton, Canada

Abstract

In this article, a novel multilateral teleoperation structure is presented for cooperative control of a redundant remote robot in the task-space. In the structure, each local robot is assigned a real number between zero and one, as its dominance factor. The sum of all the assigned factors is equal to one, and a greater dominance factor implies that its corresponding operator will have more power in controlling the remote robot. The time-varying delays in the communication channels, the actuators saturation, and the nonlinear dynamics are incorporated into the controller development. Using Barbalat's lemma and a Lyapunov-Krasovskii functional, the asymptotic stability analysis of the closed-loop dynamics are shown, and the performance claims are delivered. Simulation and experimental results are provided to verify the theoretical findings.

Keywords: Cooperative control, multilateral teleoperation, saturation control, task-space synchronization, time-varying delay

1. Introduction

A general teleoperation system is composed of local (master) and remote (slave) robots where the controlled coupling between them makes the remote robots to be under the control of operators who manipulate the local robots. Given that the physical presence of operators in unsafe or hazardous environments may put their lives at risk, teleoperation systems can provide a stable interaction with remote environments for operators to accomplish tasks without any direct manipulation. Teleoperation systems have broad application across a range of disciplines including outer-space manipulation, navigating a nuclear reactor station, defusing a bomb, undersea exploration, remote medical operation, haptics-assisted training, telerehabilitation and beyond [1]. The distance between robots renders the exchanged signals delayed which can destabilize and degrade the system performance [2, 3].

The stability analysis of teleoperation systems with constant time delays have been extensively studied using wave-variable or scattering formulation [4, 5]. Also, PD-like controllers [6] as well as control techniques based on passivity [7] and neural networks [8] have been used to achieve tracking and synchronization. Practically speaking, the delay in the forward and backward communication paths between the operator and the remote environment can be time-varying and asymmetric [9, 10]. For instance, problems like data congestion and bandwidth limitations of communication networks lead to time-varying delays which can compromise the system's performance substantially [11, 12, 13]. To counter the effect of time-varying delays, a number of control schemes have been proposed in the literature. In [14], an LMI stability analysis has been adopted for a proportional plus damping injection controller in a teleoperation system with time-varying delays. In the presence of time-varying communication delays, a control algorithm for force-reflecting teleoperation system is presented in [15]. In [16], the scattering transformation has been tailored to stability analysis of teleoperation system subject to time-varying delays. A passive control scheme is proposed for a bilateral teleoperation with time-varying communication delays and external forces [12]. Also, P+D and PD like controllers are used widely to guarantee asymptotic stability and synchronization of teleoperation systems with time-varying delays [17, 18, 19].

In practice, the amplitudes of control signals are capped by the torques that the actuators can supply. In other words, they are subject to saturation. This limitation should be taken into account in the controller design; otherwise, it may render unintended responses and even the system's instability [20]. In [21], a robust adaptive model reference impedance controller is developed for an n-link robotic manipulator with parameter uncertainties, actuator saturation, and imprecise force sensor measurement. In the realm of teleoperation systems, recently some strides have been made in addressing saturation. In [22], a nonlinear proportional control scheme incorporated with wave variable is proposed to handle actuator saturation in a delayed teleoperation. In [23], the synthesis of anti-windup approach and wave variables is put forth for constant-delay teleoperation subjected to bounded control signals. The work in [24] introduces the nP+D controller by which addresses the stability and joint-space synchronization problem of the bilateral teleoperation system subject to actuator saturation and time-varying delays. In [25], an adaptive switching-based control framework is

*Corresponding author (Fax: +98-41-33300819)
Email addresses: hashemzadeh@tabrizu.ac.ir (Farzad Hashemzadeh), ali.torabi@ualberta.ca (Ali Torabi), mahdi.tavakoli@ualberta.ca (Mahdi Tavakoli)

developed for joint-space synchronization problem of nonlinear teleoperation system with taking account of actuator saturation and asymmetric time-varying delays. In [26], a joint-space formation control problem for delayed multi-slave cyber-physical teleoperating systems with actuator saturation is investigated. In [27], to address the finite-time joint-space tracking control problem for nonlinear teleoperation systems, the anti-windup control framework is adopted and a modified anti-windup compensator is developed to analyze and handle the actuator saturation. In [28], an adaptive nonlinear fractional power proportional+damping control scheme is designed to address the joint-space synchronization control problem of flexible telerobotics with input saturation. In [29], the domain of attraction is analyzed for bilateral teleoperator subject to interval delay and saturated proportional joint-space position error plus damping injection (saturated P+D) control scheme.

In practice, most of the tasks performed remotely involve the manipulation of the end-effectors. Therefore, the study of teleoperation systems in task-space is of great practical importance to the researchers and has caught on recently. The work in [30] studies teleoperation of redundant manipulators where the robots are geared up to track a desired trajectory in task-space. However, in the controller design, the robots are assumed to have the same degrees of freedom, and the communication delays are not taken into account. In [31], ignoring the communication delays, the study proposes a teleoperation framework in which two local robots can be utilized to control different coordinates assigned to the remote robot. In [32], an adaptive semi-autonomous control framework is proposed to deal with bilateral teleoperation in which asymmetric constant communication delays are considered and the redundancy of the remote robot is utilized to achieve a sub-task control. In [33], a controller for heterogeneous bilateral teleoperation systems have been proposed to ensure stability and tracking performance in the presence of time-varying communication delays. In [34], a switching technique-based adaptive semi-autonomous control is proposed to address the task-space bilateral teleoperation system with asymmetric time-varying delays and dead-zone nonsmooth nonlinearity in the actuators of the robots. In [35], a nonlinear robust adaptive bilateral impedance controller is proposed to guarantee the force and position tracking performance, and the absolute stability of multi-DoF delayed teleoperation systems. In [36], a (nP+D)-like controller has been put forward to tackle the problem of task-space synchronization for nonlinear bilateral teleoperation in the presence of actuators saturation and time-varying delays. In [37], an adaptive switching-based control framework is investigated for task-space performance in teleoperation system with asymmetric time-varying delays.

Unlike the bilateral teleoperation systems which consist of one local robot and one remote robot, the multilateral teleoperation frameworks involve a minimum of three robots in order to remotely perform a task [38]. Given that many practical tasks are completed by several robots, various frameworks have been geared up to deliver the multilateral teleoperation. Frameworks mainly include Single-Master/Multiple-Slave [39, 40, 41, 42, 43], Multiple-Master/Multiple-Slave [44, 45, 46, 47, 48, 49], and Multiple-Master/Single-Slave [50, 51, 52, 53, 54] configurations.

As far as the multilateral cooperative nonlinear teleoperation with a solitary remote robot is concerned, in [50] a PD-like controller is proposed to guarantee stability and asymptotic joint-position tracking of nonlinear dual-user teleoperation in the presence of time-varying communication delays. In [51], a nonlinear trilateral model reference adaptive impedance controller is presented for nonlinear dual-user multi-DoF teleoperation systems and it is shown that different performance goals such as Cartesian position synchronization and force reflection can be achieved via different adjustments to the impedance parameters. In [52], the nP+D controller is developed for joint-space synchronization problem of dual-user trilateral nonlinear teleoperation subjected to time-varying delays and actuator saturation. In [53], in the presence of constant time delays, an adaptive-based neural network is developed for joint-position tracking control of dual-user trilateral teleoperation. In literature, though the dual-user trilateral teleoperation is subsumed under the Multi-Master/Single-Slave teleoperation, the latter has received very little attention. In [54], an impedance-based control methodology is developed for MM/SS teleoperation to satisfy desired tracking and force-reflection in the presence of time delays. In Multi-Master teleoperations, a parameter namely 'dominance factor' is commonly utilized to regulate the interactions between operators and their authority over the task operation [49, 50, 52, 53, 54].

In this paper, a novel cooperative control architecture is proposed for multilateral multi-user teleoperation system which enables several operators to cooperatively control a redundant remote manipulator in the task-space. The proposed scheme splits the control process between all local operators whose dominance in manipulating the remote robot are determined by their relevant assigned dominance factors which are real numbers between 0 and 1. A bigger dominance factor for a local robot means its corresponding operator will have a larger influence on the movement of the remote robot and will have the upper hand over the other operators in controlling the remote robot. Also, in contact motion, it is shown that there is a relationship between the reflected force from the environment and all the applied forces on the local robots. As the pertinent works go, the main contributions of this paper are sumed up as follows.

- Through the developed method, desired objectives can be achieved in the simultaneous presence of the actuators saturation, the nonlinearity in the dynamics, and time-varying delays in the communication channels.

- In contrast to [54], in which it is assumed that the operators and their relevant operators should be located at the same site, using our proposed framework and controller, the operators can manipulate from various locations.

- In [54], the reflected force from the environment needs to pass through a lowpass filter before reaching the operators' side, which inevitably mitigates the high-frequency component of the reflected force, compromising the desired transparency. In our proposed framework, the position signals can directly be transferred between the robots.

- In contrast to [49, 50, 52, 53, 54], in which the dominance factor is considered to be a scalar parameter, we have studied the dominance factor respecting the dimension of the task-space.
- In contrast to [54], in the proposed controller, the sub-task control has also been taken into account. To lay the foundation for a sub-task control such as singularity avoidance, the redundancy of the remote robot has been incorporated into the controller development.

Using Barbalat's lemma and a Lyapunov-Krasovskii functional, the asymptotic stability analysis of the closed-loop dynamics is given to substantiate the boundedness of error signals in contact motion and full synchronization of the task-space positions in free motion. The efficiency of the proposed control algorithm is verified by showing a number of numerical simulations and experimental results.

This paper is organized in sections as follows. Section 2 gives problem formulation and preliminaries while stability analysis is studied in Section 3. In Section 4 sub-task control and in Section 5 simulation and experimental results are discussed. In Sections 6 and 7, conclusion and appendix are presented, respectively.

Throughout this paper, we indicate the set of real numbers by $\mathbb{R}=(-\infty,\infty)$ and the set of positive real numbers by $\mathbb{R}_{>0}=(0,\infty)$. The L_∞ and L_2 norms of a time function $f:\mathbb{R}_{\geq 0}\to\mathbb{R}^{n\times 1}$ are shown as $\|f\|_{L_\infty}=\sup_{t\in[0,\infty)}\|f\|_\infty$ and $\|f\|_{L_2}=\sqrt{\int_0^\infty \|f\|_2^2 dt}$, respectively. The L_∞ and L_2 spaces are defined as the sets of $\{f:\mathbb{R}_{\geq 0}\to\mathbb{R}^{n\times 1}, \|f\|_{L_\infty}<+\infty\}$ and $\{f:\mathbb{R}_{\geq 0}\to\mathbb{R}^{n\times 1}, \|f\|_{L_2}<+\infty\}$, respectively. For clarity, we refer to $\|f\|_{L_\infty}$ as $\|f\|_\infty$ and to $\|f\|_{L_2}$ as $\|f\|_2$. Also, the notation $\lim_{t\to\infty} f(t)=0$ is made concise by the notation $f\to 0$, and the argument of time-dependent signals are left out unless they are required for the sake of clarity.

2. Problem Formulation and Preliminaries

In this section, we formulate the multilateral teleoperation system in such a way as to make it possible for multiple operators to control the remote robot's end-effector cooperatively. In the proposed framework, the task-space positions are mutually exchanged between all the robots (see Figure 1). Therefore, the position signals are the only signals exchanged between the robots. Each local robot is assigned a dominance factor which determines how effective its corresponding operator can handle the remote robot. We assume that the outgoing signals of each robot are subject to continuous time-varying delays when traveling through the communication channel. In other words, in the proposed framework, the exchanged signals pass through such communication channels that the continuity of time-varying delays is guaranteed (Assumption 1). The cooperative performance of the system is defined in the shape of the error signals, and the task objectives are claimed as Theorems 1-3.

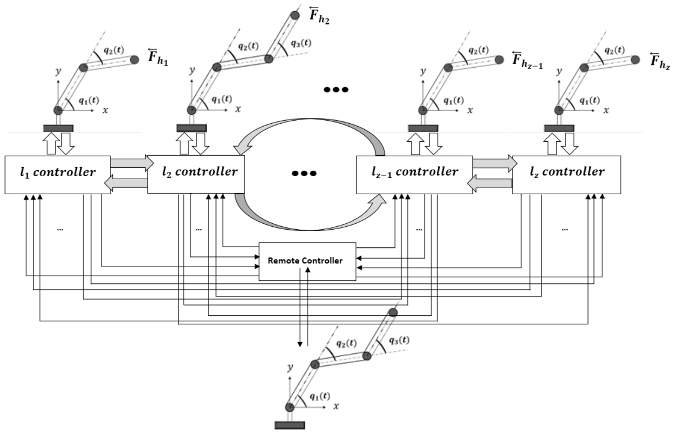

Figure 1: The proposed multilateral framework for cooperative control of the redundant remote robot, the end-effector positions are mutually exchanged between all robots through time-varying delays.

2.1. System Dynamics and Saturation Model

Consider the manipulators in the multilateral teleoperation system as Lagrangian systems whose control signals are subject to saturation. With the assumption that the manipulators are driven by actuated revolute joints, let us represent the dynamics of the local (l) and remote (r) robots as

$$M_k(q_k)\ddot{q}_k+C_k(q_k,\dot{q}_k)\dot{q}_k+G_k(q_k)=\tau_{e_k}+S_k(\tau_k) \tag{1}$$

where for $k\in\{r,\bigcup_{\dagger=1}^{z} l_\dagger\}$, the notations $q_k\in\mathbb{R}^{\beta_k\times 1}$, $\dot{q}_k\in\mathbb{R}^{\beta_k\times 1}$ and $\ddot{q}_k\in\mathbb{R}^{\beta_k\times 1}$ are the vectors of the joint positions, velocities and accelerations of the robots, respectively. Note that $l_\dagger$ denotes the $\dagger^{th}$ local robot and $z\geq 2$ denotes the number of robots in the local site. Also, $\beta_{l_\dagger}=n_\dagger$ and $\beta_r=m$ denote the number of joints in the $\dagger^{th}$ local robot and the remote robot, respectively. $M_k(q_k)\in\mathbb{R}^{\beta_k\times\beta_k}$, $C_k(q_k,\dot{q}_k)\in\mathbb{R}^{\beta_k\times\beta_k}$ and $G_k(q_k)\in\mathbb{R}^{\beta_k\times 1}$ are the inertia matrix, the Coriolis/centrifugal matrix and the gravitational vector, respectively. Moreover, $\tau_{e_k}\in\mathbb{R}^{\beta_k\times 1}$ denotes the exerted torques on the robots' joints, and $\tau_k\in\mathbb{R}^{\beta_k\times 1}$ denotes their control signals. Also, the saturation of the control signals are modeled by vector function $S_k(\tau_k):\mathbb{R}^{\beta_k\times 1}\to\mathbb{R}^{\beta_k\times 1}$ whose elements; $s_{k_i}(\tau_{k_i}):\mathbb{R}\to\mathbb{R}$, $i=1,\ldots,\beta_k$, are defined as follows

$$s_{k_i}(\tau_{k_i})=\begin{cases} B_{k_i} & \text{if} \quad \tau_{k_i}>B_{k_i} \\ \tau_{k_i} & \text{if} \quad |\tau_{k_i}|\leq B_{k_i} \\ -B_{k_i} & \text{if} \quad \tau_{k_i}<-B_{k_i} \end{cases} \tag{2}$$

where $B_{k_i}\in\mathbb{R}_{>0}$ is the saturation level of the corresponding actuator and τ_{k_i} denotes the control signal applied on the i^{th} joint of the corresponding robot. It is imperative to have $0<\Omega_{k_i}<B_{k_i}$ where $|g_{k_i}(q_k)|\leq\Omega_{k_i}$, and $g_{k_i}(q_k)$ is the i^{th} element of the gravity vector $G_k(q_k)$. This condition implies that the actuators of the manipulators are capable of overcoming the gravity of corresponding robots within their workspaces.

2.2. Error Signals

Let $X_k\in\mathbb{R}^{\varepsilon\times 1}$ represent the positions of the robots in the task-space and ε denote the dimension of the task-space. The relation between the task-space positions and the joint-space positions of the robots are as

$$X_k = h_k(q_k), \quad \dot{X}_k = J_k(q_k)\dot{q}_k \tag{3}$$

where $h_k(q_k):\mathbb{R}^{\beta_k\times 1}\rightarrow\mathbb{R}^{\varepsilon\times 1}$ describes the nonlinear mapping between the joint-space positions and the task-space positions, and $J_k(q_k)\in\mathbb{R}^{\varepsilon\times\beta_k}$ is the Jacobian matrix defined as $J_k(q_k)=\frac{\partial h_k(q_k)}{\partial q_k}$. Given that the dominance factor $\Pi_\dagger$ is assigned to the $\dagger^{th}$ local robot, the task-space position errors are defined as

$$\begin{cases} e_{l_\dagger} \triangleq X_{l_\dagger}(t) - \Pi_\dagger X_r(t-d_{r\dagger}(t)) - \sum\limits_{\nu=1;\nu\neq\dagger}^{z} \Pi_\nu X_{l_\nu}(t-d_{\nu\dagger}(t)) \\ e_{l_\dagger}^0 \triangleq X_{l_\dagger}(t) - \Pi_\dagger X_r(t) - \sum\limits_{\nu=1;\nu\neq\dagger}^{z} \Pi_\nu X_{l_\nu}(t) \\ e_r \triangleq X_r(t) - \sum\limits_{\dagger=1}^{z} \Lambda_\dagger X_{l_\dagger}(t-d_{\dagger r}(t)) \\ e_r^0 \triangleq X_r(t) - \sum\limits_{\dagger=1}^{z} \Lambda_\dagger X_{l_\dagger}(t) \end{cases} \tag{4}$$

where $\Lambda_\dagger \triangleq \Pi_\dagger^2 / \sum\limits_{\dagger=1}^{z}\Pi_\dagger^2$, $\sum\limits_{\dagger=1}^{z}\Pi_\dagger = \sum\limits_{\dagger=1}^{z}\Lambda_\dagger = 1$ and $\Pi_\dagger = 1 - \sum\limits_{\nu=1;\nu\neq\dagger}^{z}\Pi_\nu$ such that $0<\Pi_\dagger,\Lambda_\dagger,\Pi_\nu\in\mathbb{R}<1$. Also, $d_{r\dagger}(t)$ and $d_{\dagger r}(t)$ are backward (from the remote robot to the $\dagger^{th}$ local robot) and forward (from the $\dagger^{th}$ local robot to the remote robot) time-varying delays between the local and remote robots. Also, $d_{\nu\dagger}(t)$ denotes the time-varying delay from the ν^{th} local robot to the $\dagger^{th}$ local robot.

For the sake of simplicity, in the rest of the paper, the notations M_k, M_k^{-1}, C_k, C_k^T, G_k, J_k, J_k^T and J_r^+ are used instead of $M_k(q_k)$, $M_k^{-1}(q_k)$, $C_k(q_k,\dot{q}_k)$, $C_k^T(q_k,\dot{q}_k)$, $G_k(q_k)$, $J_k(q_k)$, $J_k^T(q_k)$ and $J_r^+(q_r)$ ($\mathbb{R}^{m\times 1}\rightarrow\mathbb{R}^{m\times\varepsilon}$, being the pseudo-inverse of $J_r(q_r)$ defined later), respectively. Also, q_{k_i}, $\dot{q}_{k_i}$ and g_{k_i} are the i^{th} element (coressponding to the i^{th} joint) of the vectors q_k, $\dot{q}_k$ and G_k, respectively.

2.3. Dynamics Modification for Sub-Task Control

Inspired by [55, 32], let us reformulate the robots' dynamics in order to incorporate the sub-task control into the controller development. To this end, first consider the signals $\zeta_k\in\mathbb{R}^{\beta_k\times 1}$ and $\varphi_k\in\mathbb{R}^{\beta_k\times 1}$ defined as

$$\varphi_k \triangleq \dot{q}_k - \zeta_k; \qquad \zeta_k \triangleq \begin{cases} 0 & \text{if} \quad k=l_\dagger \\ (\mathbb{I}_m - J_r^+ J_r)\Psi_r & \text{if} \quad k=r \end{cases} \tag{5}$$

where $\Psi_r\in\mathbb{R}^{m\times 1}$ is the negative gradient of an appropriately defined function for the sub-task control, and $\mathbb{I}_m$ is the identity matrix of size m. Also, $J_r^+\in\mathbb{R}^{m\times\varepsilon}$ is the pseudo-inverse of J_r defined by $J_r^+ \triangleq J_r^T(J_r J_r^T)^{-1}$ which satisfies $J_r J_r^+ = \mathbb{I}_m$ and $J_r(\mathbb{I}_m - J_r^+ J_r)=0$, and accordingly $J_r(\mathbb{I}_m - J_r^+ J_r)\Psi_r = 0$ which in turn implies that $(\mathbb{I}_m - J_r^+ J_r)$ projects the vector Ψ_r onto the null space of J_r. Therefore, if the link velocity in the null space of J_r is such that tracks $(\mathbb{I}_m - J_r^+ J_r)\Psi_r$, then not only it will not influence the task-space motion, but also it can be regulated by Ψ_r. Now, taking the derivative of the both sides of the equation $\varphi_k = \dot{q}_k - \zeta_k$ with respect to time, premultiplying them by the inertia matrix M_k and substituting $M_k\ddot{q}_k$ with its equivalent from (1), the robots' modified dynamics can be derived as

$$M_k\dot{\varphi}_k + C_k\varphi_k = \Theta_k + \tau_{e_k} + S_k(\tau_k) \tag{6}$$

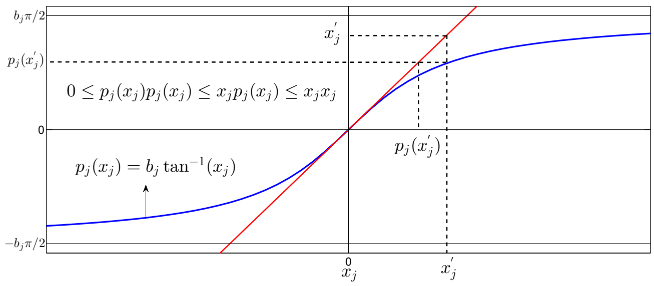

Figure 2: The nonlinear function used in the proposed controller.

where $\Theta_k\in\mathbb{R}^{\beta_k\times 1} \triangleq -M_k\dot{\zeta}_k - C_k\zeta_k - G_k$ and $\tau_{e_k} = J_k^T F_{e_k}$. Furthermore, let $\theta_{k_i}\in\mathbb{R}$; $i=1,\ldots,\beta_k$, be the elements of the vector Θ_k. Note that $\Theta_{l_\dagger} = -G_{l_\dagger}$, and $F_{e_k}\in\mathbb{R}^{\varepsilon\times 1}$ denotes the force vectors exerted on the end-effectors of the robots.

2.4. Proposed Controller

Given the modified dynamical system (6), the control signals are designed as

$$\tau_k = -\Theta_k - J_k^T \Phi P_k(.) - \Sigma_k\varphi_k \tag{7}$$

where

$$\begin{cases} P_{l_\dagger}(.) \triangleq \Pi_\dagger P(e_{\dagger r}) + \sum\limits_{\nu=1;\nu\neq\dagger}^{z}\Pi_\nu P(e_{\dagger\nu}) \\ e_{\dagger r} \triangleq X_{l_\dagger}(t) - X_r(t-d_{r\dagger}(t)); \quad e_{\dagger\nu} \triangleq X_{l_\dagger}(t) - X_{l_\nu}(t-d_{\nu\dagger}(t)) \\ P_r(.) \triangleq \sum\limits_{\dagger=1}^{z}\Pi_\dagger^2 P\Big(X_r(t) - X_{l_\dagger}(t-d_{\dagger r}(t))\Big) \triangleq \sum\limits_{\dagger=1}^{z}\Pi_\dagger^2 P(e_{r\dagger}) \end{cases} \tag{8}$$

Also, $\Sigma_k\in\mathbb{R}^{\beta_k\times\beta_k}$ and $\Phi\in\mathbb{R}^{\varepsilon\times\varepsilon}$ are positive-definite diagonal matrices with $\sigma_{k_{i=1,\ldots,\beta_k}}\in\mathbb{R}_{>0}$ and $\phi_{j=1,\ldots,\varepsilon}\in\mathbb{R}_{>0}$ as their respective elements such that $\sigma_{k_{min}} \triangleq \min\limits_i\{\sigma_{k_i}\}$, $\sigma_{k_{max}} \triangleq \max\limits_i\{\sigma_{k_i}\}$, and $\phi_{max} \triangleq \max\limits_j\{\phi_j\}$. For any $x_j\in\mathbb{R}$ and $X\in\mathbb{R}^{\varepsilon\times 1}$, $P(X):R^{\varepsilon\times 1}\rightarrow R^{\varepsilon\times 1}$ is a nonlinear vector function with elements $p_j(x_j):\mathbb{R}\rightarrow\mathbb{R}$; $j=1,\ldots,\varepsilon$, which are required to be strictly increasing, passing through the origin, bounded, continuous, concave for positive x_j and convex for negative x_j with continuous first derivative around the origin such that $0\leq x_j p_j(x_j)\leq x_j x_j$, $|p_j(x_j)|\leq|x_j|$ and $p_j(-x_j)=-p_j(x_j)$ [24]. For instance, the nonlinear function $p_j(x_j)=b_j\tan^{-1}(x_j)$; $0<b_j\leq 1$, embodies all the mentioned properties such that $\frac{\partial p_j(x_j)}{\partial x_j}$ is positive and bounded (see Figure 2). Also, let N_j be defined as $N_j \triangleq \sup p_j(x_j) = b_j\pi/2$.

2.5. Preliminaries

According to [56, 57], the following properties hold for the dynamics of the nonlinear models (1):

Property 1. *The inertia matrix $M_k\in\mathbb{R}^{\beta_k\times\beta_k}$ is symmetric positive-definite and has the following upper and lower bounds:*

$$0 < \lambda_{min}(M_k)\mathbb{I}_{\beta_k} \leq M_k \leq \lambda_{max}(M_k)\mathbb{I}_{\beta_k} < \infty$$

where $\mathbb{I}_{\beta_k}$ is the identity matrix of size β_k.

Property 2. *$\dot{M}_k - 2C_k$ is a skew symmetric matrix or $\forall\varphi_k\in\mathbb{R}^{\beta_k\times 1}$, $\varphi_k^T\Big(\dot{M}_k - 2C_k\Big)\varphi_k = 0$, to be exact.*

Property 3. *The time derivative of C_k is bounded if $\ddot{q}_k$ and $\dot{q}_k$ are bounded.*

Property 4. *The gravity vector G_k is bounded, i.e., there exist positive constants Ω_{k_i} such that every element of the gravity vector $g_{k_{i=1,\ldots,\beta_k}}$ satisfies $|g_{k_i}|\leq\Omega_{k_i}$.*

Property 5. *For a manipulator with revolute joints, there exists a positive υ bounding the Coriolis/centrifugal term as*

$$\|C_k(q_k,x)y\|_2\leq\upsilon\|x\|_2\|y\|_2.$$

Also, some assumptions are considered as follows.

Assumption 1. *The time derivative of all the time-varying delays in the communication channels are bounded.*

Assumption 2. *The operators and the environment are passive, i.e., there exist positive constants $\Pi_k,\vartheta_k<\infty$ such that*

$$\vartheta_k+\int_0^t -\Pi_k\dot{q}_k^T(\mu)\tau_{e_k}(\mu)d\mu>0 \tag{9}$$

Now, let us bring up two preliminary lemmas which are extensions of the Lemmas 3.2 and 3.3 used in [36].

Lemma 1. *The following inequalities hold (see Appendix):*

$$\dot{X}_r^T\Phi\Big(P_r^0(.)-P_r(.)\Big)\leq2\sum_{\dagger=1}^{z}\Pi_\dagger^2\big|\dot{X}_r\big|^T\Phi\int_{t-d_{\dagger r}(t)}^{t}P\Big(\big|\dot{X}_{l_\dagger}(\tau)\big|\Big)d\tau \tag{10}$$

$$\begin{aligned}\dot{X}_{l_\dagger}^T\Phi\Big(P_{l_\dagger}^0(.)-P_{l_\dagger}(.)\Big)\leq&2\sum_{\nu=1;\nu\neq\dagger}^{z}\Pi_\nu\big|\dot{X}_{l_\dagger}\big|^T\Phi\int_{t-d_{\nu\dagger}(t)}^{t}P\Big(\big|\dot{X}_{l_\nu}(\tau)\big|\Big)d\tau\\&+2\Pi_\dagger\big|\dot{X}_{l_\dagger}\big|^T\Phi\int_{t-d_{r\dagger}(t)}^{t}P\Big(\big|\dot{X}_r(\tau)\big|\Big)d\tau\end{aligned} \tag{11}$$

Lemma 2. *Adopting a similar approach used in the proof of Lemma 3.3 [36], the following inequalities hold:*

$$\big|\dot{X}_r\big|^T\Phi\int_{t-d_{\dagger r}(t)}^{t}P\Big(\big|\dot{X}_{l_\dagger}(\tau)\big|\Big)d\tau-\int_{t-d_{\dagger r}(t)}^{t}\dot{X}_{l_\dagger}^T(\tau)\Phi P\Big(\dot{X}_{l_\dagger}(\tau)\Big)d\tau\leq\bar{d}_{\dagger r}\dot{X}_r^T\Phi P\Big(\dot{X}_r\Big) \tag{12}$$

$$\begin{aligned}\sum_{\nu=1;\nu\neq\dagger}^{z}\Pi_\nu\big|\dot{X}_{l_\dagger}\big|^T\Phi\int_{t-d_{\nu\dagger}(t)}^{t}P\Big(\big|\dot{X}_{l_\nu}(\tau)\big|\Big)d\tau-\sum_{\nu=1;\nu\neq\dagger}^{z}\Pi_\nu\int_{t-d_{\nu\dagger}(t)}^{t}\dot{X}_{l_\nu}^T(\tau)\Phi P\Big(\dot{X}_{l_\nu}(\tau)\Big)d\tau\\\leq\sum_{\nu=1;\nu\neq\dagger}^{z}\Pi_\nu\bar{d}_{\nu\dagger}\dot{X}_{l_\dagger}^T\Phi P\Big(\dot{X}_{l\dagger}\Big)\end{aligned} \tag{13}$$

$$\big|\dot{X}_{l_\dagger}\big|^T\Phi\int_{t-d_{r\dagger}(t)}^{t}P\Big(\big|\dot{X}_r(\tau)\big|\Big)d\tau-\int_{t-d_{r\dagger}(t)}^{t}\dot{X}_r^T(\tau)\Phi P\Big(\dot{X}_r(\tau)\Big)d\tau\leq\bar{d}_{r\dagger}\dot{X}_{l_\dagger}^T\Phi P\Big(\dot{X}_{l_\dagger}\Big) \tag{14}$$

3. Stability Analysis

This section delineates the stability analysis of the teleoperation system (1) with the proposed controller (7). Applying the proposed controller to the modified dynamics (6), the next formula is readily found for the complete closed-loop system:

$$M_k\dot{\varphi}_k+C_k\varphi_k=\Theta_k+\tau_{e_k}+S_k\left(\underbrace{-\Theta_k-J_k^T\Phi P_k(.)-\Sigma_k\varphi_k}_{\triangleq\Delta_k}\right) \tag{15}$$

Now, using Lyapunov–Krasovskii functionals method, the following theorem is proved.

Theorem 1. *Assume that the Jacobian matrices of the local manipulators are full rank, and all the time-varying delays in the communication channels are bounded. Also, the operators and the environment are passive. In the multilateral teleoperation system (1) with the introduced controller (7), the end-effector velocities $\dot{X}_k$ and the task-space position errors; e_k and e_k^0 (4), are bounded as long as the following conditions are maintained.*

1. $\sigma_{k_{min}}\geq\frac{2\beta_kT_k\phi_{max}J_{k_{max}}^{(2)}}{\Pi_k}$
2. $\phi_{max}\leq\min\limits_k\left\{\frac{\omega_k\left(B_{k_{min}}-\Omega_{k_{max}}-\Upsilon_k\right)}{\varepsilon N_{max}J_{k_{max}}\Xi_k(4d_{max}+\omega_k)}\right\}$

where $J_{k_{max}}^{(2)}\triangleq\max\limits_{i\alpha}\left\{\sup\left|J_{k_{i\alpha}}^{(2)}\right|\right\}_{i,\alpha=1,\ldots,\beta_k}$ such that $J_k^{(2)}\triangleq J_k^TJ_k$ and $J_{k_{i\alpha}}^{(2)}$ are the elements of the $J_k^{(2)}$ matrix. Also, $\Xi_r\triangleq\sum\limits_{\dagger=1}^{z}\Pi_\dagger^2$, $\Xi_{k\neq r}\triangleq\sum\limits_{\dagger=1}^{z}\Pi_\dagger=1$, $\Upsilon_k\triangleq\max\limits_i\left\{\left|\sum\limits_{\alpha=1}^{\beta_k}\left(M_{k_{i\alpha}}\dot{\zeta}_{k_\alpha}+C_{k_{i\alpha}}\zeta_{k_\alpha}\right)\right|\right\}$, $J_{k_{max}}\triangleq\max\limits_{ji}\left\{\sup\left|J_{k_{ji}}\right|\right\}$. Note that $J_{k_{ji}}$ are the elements of the matrix J_k such that $j=1,\ldots,\varepsilon$ and $i=1,\ldots,\beta_k$. Also, $N_{max}\triangleq\max\limits_j\{N_j\}$, $B_{k_{min}}\triangleq\min\limits_i\{B_{k_i}\}$ and $\Omega_{k_{max}}\triangleq\max\limits_i\{\Omega_{k_i}\}$. Moreover, $M_{k_{i\alpha}},C_{k_{i\alpha}}\in\mathbb{R}$ are the elements of the M_k and C_k matrices, respectively, in which $i,\alpha=1,\ldots,\beta_k$. Also, $\dot{\zeta}_{k_\alpha},\zeta_{k_\alpha}\in\mathbb{R}$ are the elements of the vectors $\dot{\zeta}_k$ and ζ_k, respectively. Furthermore, $\Pi_r=1$, $\Pi_{l_\dagger}\triangleq\Pi_\dagger$, $\omega_k\triangleq\frac{\sigma_{k_{min}}}{\sigma_{k_{max}}}$ and T_k is total round-trip delay defined as

$$T_k\triangleq\begin{cases}\sum\limits_{\dagger=1}^{z}\Pi_\dagger^2\Big(\bar{d}_{r\dagger}+\bar{d}_{\dagger r}\Big) & if\quad k=r\\ \Pi_\dagger^2\Big(\bar{d}_{r\dagger}+\bar{d}_{\dagger r}\Big)+\sum\limits_{\nu=1;\nu\neq\dagger}^{z}\Pi_\dagger\Pi_\nu\Big(\bar{d}_{\nu\dagger}+\bar{d}_{\dagger\nu}\Big) & if\quad k=l_\dagger\end{cases} \tag{16}$$

where $\bar{d}_{r\dagger}\triangleq\max\{d_{r\dagger}(t)\}$, $\bar{d}_{\dagger r}\triangleq\max\{d_{\dagger r}(t)\}$, $\bar{d}_{\nu\dagger}\triangleq\max\{d_{\nu\dagger}(t)\}$ and $\bar{d}_{\dagger\nu}\triangleq\max\{d_{\dagger\nu}(t)\}$. Also, $d_{max}\triangleq\max\left\{\bigcup\limits_{\dagger=1}^{z}\left\{\bar{d}_{r\dagger},\bar{d}_{\dagger r},\bigcup\limits_{\nu=\dagger+1}^{z}\left\{\bar{d}_{\dagger\nu},\bar{d}_{\nu\dagger}\right\}\right\}\right\}$ is the maximum delay in the communication channels.

Proof. To investigate the stability of the closed-loop system (15) let $x_t=x(t+\varrho)$ represent the state of the system [7, 58] where $x(t)\triangleq[\varphi_{l_1}\ \ldots\ \varphi_{l_z}\ \varphi_r\ X_{l_1}\ \ldots\ X_{l_z}\ X_r\ \dot{X}_{l_1}\ \ldots\ \dot{X}_{l_z}\ \dot{X}_r]$ and $-d_{max}\leq\varrho\leq0$. Now, consider the following Lyapunov-Krasovskii functional $V(x_t)=\sum\limits_{u=1}^{3}V_u(x_t)$ where

$$V_1(x_t)=\sum_k\left(\frac{1}{2}\Pi_k\varphi_k^TM_k\varphi_k+\int_0^t-\Pi_k\dot{q}_k^T(\mu)\tau_{e_k}(\mu)d\mu+\vartheta_k\right) \tag{17}$$

$$V_2(x_t)=\sum_{\dagger=1}^{z}\left(\sum_{\nu=\dagger+1}^{z}\left(\sum_{j=1}^{\varepsilon}\int_0^{X_{l_{\dagger j}}-X_{l_{\nu j}}}\Pi_\dagger\Pi_\nu\phi_j p_j(\gamma_j)d\gamma_j\right)\right.$$
$$\left.+\sum_{\nu=1;\nu\neq\dagger}^{z}\left(\sum_{j=1}^{\varepsilon}\int_0^{X_{l_{\dagger j}}-X_{r_j}}\Pi_\dagger(\frac{1}{z-1}-\Pi_\nu)\phi_j p_j(\gamma_j)d\gamma_j\right)\right) \tag{18}$$

$$V_3(x_t)=2\sum_{\dagger=1}^{z}\left(\Pi_\dagger^2\int_{-\bar{d}_{\dagger r}}^{0}\int_{t+\gamma}^{t}\dot{X}_{l_\dagger}^T(\tau)\Phi P\left(\dot{X}_{l_\dagger}(\tau)\right)d\tau d\gamma\right.$$
$$+\sum_{\nu=1;\nu\neq\dagger}^{z}\Pi_\dagger\Pi_\nu\int_{-\bar{d}_{\nu\dagger}}^{0}\int_{t+\gamma}^{t}\dot{X}_{l_\nu}^T(\tau)\Phi P\left(\dot{X}_{l_\nu}(\tau)\right)d\tau d\gamma \tag{19}$$
$$\left.+\Pi_\dagger^2\int_{-\bar{d}_{r\dagger}}^{0}\int_{t+\gamma}^{t}\dot{X}_r^T(\tau)\Phi P\left(\dot{X}_r(\tau)\right)d\tau d\gamma\right)$$

Given Assumption 2, Property 2, the closed-loop dynamics (15) and the facts that $\tau_{e_k}=J_k^T F_{e_k}$, $\zeta_k^T J_k^T=0$, $\varphi_k^T\tau_{e_k}=\dot{q}_k^T\tau_{e_k}$ and $\varphi_k^T J_k^T=\dot{X}_k^T$, and defining $D_k\triangleq\Pi_k\dot{X}_k^T\Phi P_k(.)$ and $D_k^{'}\triangleq-\Pi_k\dot{X}_k^T\Phi P_k(.)$ such that $D_k+D_k^{'}=0$, we have

$$\dot{V}_1(x_t)+\sum_k D_k=\sum_k\Pi_k\varphi_k^T(S_k(\Delta_k-\Sigma_k\varphi_k)-\Delta_k) \tag{20}$$

Defining $\delta_k\triangleq\frac{-\Pi_k}{\varphi_k^T\Sigma_k\varphi_k}\varphi_k^T(S_k(\Delta_k-\Sigma_k\varphi_k)-\Delta_k)$ and substituting it into (20) we get $\dot{V}_1(x_t)+\sum_k D_k=-\sum_k\delta_k\varphi_k^T\Sigma_k\varphi_k$. Deriving the time derivative of $V_2(x_t)$ as $\dot{V}_2(x_t)=\sum_k\Pi_k\dot{X}_k^T\Phi P_k^0(.)$ such that

$$\begin{cases}P_{l_\dagger}^0(.)\triangleq\Pi_\dagger P(e_{\dagger r}^0)+\sum_{\nu=1;\nu\neq\dagger}^{z}\Pi_\nu P\left(e_{\dagger\nu}^0\right)\\ e_{\dagger r}^0\triangleq X_{l_\dagger}(t)-X_r(t);\quad e_{\dagger\nu}^0\triangleq X_{l_\dagger}(t)-X_{l_\nu}(t)\\ P_r^0(.)\triangleq\sum_{\dagger=1}^{z}\Pi_\dagger^2 P\left(X_r(t)-X_{l_\dagger}(t)\right)\triangleq\sum_{\dagger=1}^{z}\Pi_\dagger^2 P\left(e_{r\dagger}^0\right)\end{cases} \tag{21}$$

and using Lemma 1, we get

$$\dot{V}_2(x_t)+\sum_k D_k^{'}\leq 2\sum_{\dagger=1}^{z}\left(\Pi_\dagger^2\left|\dot{X}_r\right|^T\Phi\int_{t-d_{\dagger r}(t)}^{t}P\left(\left|\dot{X}_{l_\dagger}(\tau)\right|\right)d\tau\right.$$
$$+\left(\sum_{\nu=1;\nu\neq\dagger}^{z}\Pi_\dagger\Pi_\nu\left|\dot{X}_{l_\dagger}\right|^T\Phi\int_{t-d_{\nu\dagger}(t)}^{t}P\left(\left|\dot{X}_{l_\nu}(\tau)\right|\right)d\tau\right) \tag{22}$$
$$\left.+\Pi_\dagger^2\left|\dot{X}_{l_\dagger}\right|^T\Phi\int_{t-d_{r\dagger}(t)}^{t}P\left(\left|\dot{X}_r(\tau)\right|\right)d\tau\right)$$

Obtaining the time derivative of $V_3(x_t)$ as

$$\dot{V}_3(x_t)\leq 2\sum_{\dagger=1}^{z}\left(\Pi_\dagger^2\left(\bar{d}_{\dagger r}\dot{X}_{l_\dagger}^T\Phi P\left(\dot{X}_{l_\dagger}\right)-\int_{t-d_{\dagger r}(t)}^{t}\dot{X}_{l_\dagger}^T(\tau)\Phi P\left(\dot{X}_{l_\dagger}(\tau)\right)d\tau\right)\right.$$
$$+\sum_{\nu=1;\nu\neq\dagger}^{z}\Pi_\dagger\Pi_\nu\left(\bar{d}_{\nu\dagger}\dot{X}_{l_\nu}^T\Phi P\left(\dot{X}_{l_\nu}\right)-\int_{t-d_{\nu\dagger}(t)}^{t}\dot{X}_{l_\nu}^T(\tau)\Phi P\left(\dot{X}_{l_\nu}(\tau)\right)d\tau\right) \tag{23}$$
$$\left.+\Pi_\dagger^2\left(\bar{d}_{r\dagger}\dot{X}_r^T\Phi P\left(\dot{X}_r\right)-\int_{t-d_{r\dagger}(t)}^{t}\dot{X}_r^T(\tau)\Phi P\left(\dot{X}_r(\tau)\right)d\tau\right)\right)$$

and adding (23) to (22), and using Lemma 2 results in

$$(23)+(22)\leq 2\sum_{\dagger=1}^{z}\left(\left(\Pi_\dagger^2\left(\bar{d}_{\dagger r}+\bar{d}_{r\dagger}\right)+\sum_{\nu=1;\nu\neq\dagger}^{z}\Pi_\dagger\Pi_\nu\bar{d}_{\nu\dagger}\right)\dot{X}_{l_\dagger}^T\Phi P\left(\dot{X}_{l_\dagger}\right)\right.$$
$$\left.+\left(\sum_{\nu=1;\nu\neq\dagger}^{z}\Pi_\dagger\Pi_\nu\bar{d}_{\nu\dagger}\dot{X}_{l_\nu}^T\Phi P\left(\dot{X}_{l_\nu}\right)\right)+\Pi_\dagger^2\left(\bar{d}_{r\dagger}+\bar{d}_{\dagger r}\right)\dot{X}_r^T\Phi P\left(\dot{X}_r\right)\right) \tag{24}$$
$$=\sum_k 2T_k\dot{X}_k^T\Phi P\left(\dot{X}_k\right)$$

Finally, adding (20) to (24), we get

$$\sum_{u=1}^{3}\dot{V}_u(x_t)\leq\sum_k\left(2T_k\dot{X}_k^T\Phi P\left(\dot{X}_k\right)-\delta_k\varphi_k^T\Sigma_k\varphi_k\right)$$
$$\leq\sum_k\left(2T_k\phi_{max}\dot{X}_k^T P\left(\dot{X}_k\right)-\delta_k\sigma_{k_{min}}\varphi_k^T\varphi_k\right) \tag{25}$$

Now, using $\psi_k\triangleq\frac{\dot{X}_k^T P(\dot{X}_k)}{\|\varphi_k\|_2^2}$ and substituting it into (25) leads to

$$\sum_{u=1}^{3}\dot{V}_u(x_t)\leq-\sum_k(\delta_k\sigma_{k_{min}}-2T_k\phi_{max}\psi_k)\varphi_k^T\varphi_k \tag{26}$$

From (26), a sufficient condition for $\dot{V}(x_t)\leq 0$ is

$$\delta_k\sigma_{k_{min}}\geq 2T_k\phi_{max}\psi_k \tag{27}$$

Given that $\delta_k=\frac{-\Pi_k}{\varphi_k^T\Sigma_k\varphi_k}\sum_{i=1}^{\beta_k}\varphi_{k_i}(s_{k_i}(\Delta_{k_i}-\sigma_{k_i}\varphi_{k_i})-\Delta_{k_i})$ where $\Delta_{k_i}\triangleq-\theta_{k_i}-\sum_{j=1}^{\varepsilon}J_{k_{ji}}\phi_j p_{k_j}(.)$ and $-\theta_{k_i}\triangleq g_{k_i}+\sum_{\alpha=1}^{\beta_k}\left(M_{k_{i\alpha}}\dot{\zeta}_{k_\alpha}+C_{k_{i\alpha}}\zeta_{k_\alpha}\right)$, and $p_{k_j}(.)$: $\mathbb{R}\rightarrow\mathbb{R}$ as the elements of $P_k(.)$, and the property [36] that

$$\psi_k\leq\min\left\{\beta_k J_{k_{max}}^{(2)},\frac{\sum_{i=1}^{\beta_k}\varepsilon J_{k_{max}}N_{max}|\varphi_{k_i}|}{\|\varphi_k\|_2^2}\right\} \tag{28}$$

let us find conditions under which the inequality (27) is held.

Case 1. $\left|\Delta_{k_i}-\sigma_{k_i}\varphi_{k_i}\right|\leq B_{k_i}$

Considering (2), one can get $\delta_k=\Pi_k$ and given $\psi_k\leq\beta_k J_{k_{max}}^{(2)}$ from (28), the following relation is found as a sufficient condition for $\dot{V}(x_t)\leq 0$:

$$\sigma_{k_{min}}\geq\frac{2\beta_k T_k\phi_{max}J_{k_{max}}^{(2)}}{\Pi_k} \tag{29}$$

Case 2. $|\Delta_{k_i}-\sigma_{k_i}\varphi_{k_i}|>B_{k_i}$

Because $\varphi_{k_i}(s_{k_i}(\Delta_{k_i}-\sigma_{k_i}\varphi_{k_i})-\Delta_{k_i})\leq 0$ *(see Appendix),* δ_k *can be rewritten as*

$$\delta_k=\frac{\Pi_k}{\varphi_k^T\Sigma_k\varphi_k}\sum_{i=1}^{\beta_k}|\varphi_{k_i}||s_{k_i}(\Delta_{k_i}-\sigma_{k_i}\varphi_{k_i})-\Delta_{k_i}| \tag{30}$$

Given (see Appendix)

$$|\Delta_{k_i}|<\Omega_{k_{max}}+\varepsilon\phi_{max}J_{k_{max}}\Xi_k N_{max}+\Upsilon_k \tag{31}$$

and using the reverse triangle inequality, (2) *and* (31)*, we get*

$$\begin{aligned}|s_{k_i}(\Delta_{k_i}-\sigma_{k_i}\varphi_{k_i})-\Delta_{k_i}|&\geq|s_{k_i}(\Delta_{k_i}-\sigma_{k_i}\varphi_{k_i})|-|\Delta_{k_i}|\\&>B_{k_{min}}-\Omega_{k_{max}}-\varepsilon\phi_{max}J_{k_{max}}\Xi_k N_{max}-\Upsilon_k\end{aligned} \tag{32}$$

Now, considering (30) *and using* (32)*, yields*

$$\delta_k>\sum_{i=1}^{\beta_k}\frac{\Pi_k|\varphi_{k_i}|(B_{k_{min}}-\Omega_{k_{max}}-\varepsilon\phi_{max}J_{k_{max}}\Xi_k N_{max}-\Upsilon_k)}{\sigma_{k_{max}}\|\varphi_k\|_2^2} \tag{33}$$

Using (33) *and given* $\psi_k\leq\sum_{i=1}^{\beta_k}\frac{\varepsilon J_{k_{max}}N_{max}|\varphi_{k_i}|}{\|\varphi_k\|_2^2}$ *from* (28)*, we get*

$$\delta_k\sigma_{k_{min}}\geq\frac{\sigma_{k_{min}}\Pi_k\psi_k(B_{k_{min}}-\Omega_{k_{max}}-\varepsilon\phi_{max}J_{k_{max}}\Xi_k N_{max}-\Upsilon_k)}{\varepsilon\sigma_{k_{max}}J_{k_{max}}N_{max}} \tag{34}$$

Therefore, the following relation is held as another sufficient condition for (27) *and* $\dot V(x_t)\leq 0$*:*

$$\phi_{max}\leq\min_k\left\{\frac{\omega_k(B_{k_{min}}-\Omega_{k_{max}}-\Upsilon_k)}{\varepsilon N_{max}J_{k_{max}}\left(\frac{2T_k}{\Pi_k}+\omega_k\Xi_k\right)}\right\} \tag{35}$$

Now, given that $\frac{2T_k}{\Pi_k}\leq 4d_{max}\Xi_k$ *we have the following condition by which* (35) *will be satisfied.*

$$\phi_{max}\leq\min_k\left\{\frac{\omega_k(B_{k_{min}}-\Omega_{k_{max}}-\Upsilon_k)}{\varepsilon N_{max}J_{k_{max}}\Xi_k(4d_{max}+\omega_k)}\right\} \tag{36}$$

To sum up, if (29) and (36) are satisfied, then we would have $\dot V(x_t)\leq 0$ which means all terms in $V(x_t)$ are bounded. Therefore, $\dot X_k,\varphi_k,e_k^0\in L_\infty$ and noting that

$$\begin{cases}e_{l_\dagger}=e_{l_\dagger}^0+\Pi_\dagger\int_{t-d_{r\dagger}}^{t}\dot X_r(\tau)d\tau+\sum_{\nu=1;\nu\neq\dagger}^{z}\Pi_\nu\left(\int_{t-d_{\nu\dagger}}^{t}\dot X_{l_\nu}(\tau)d\tau\right)\\ e_r=e_r^0+\sum_{\dagger=1}^{z}\Lambda_\dagger\int_{t-d_{\dagger r}}^{t}\dot X_{l_\dagger}(\tau)d\tau\end{cases} \tag{37}$$

we can conclude that $e_k\in L_\infty$. Therefore, the proof of Theorem 1 has been completed. □

Remark 1. *In a more general view, if in* (4) *and* (8) *we let* $\Pi_\dagger,\Pi_\nu,\Lambda_\dagger\in\mathbb{R}^{\varepsilon\times\varepsilon}$ *be positive-definite diagonal matrices whose elements* $0<\Pi_{\dagger_j},\Pi_{\nu_j},\Lambda_{\dagger_j}\in\mathbb{R}<1$ *satisfy in relations* $\Lambda_{\dagger_j}\triangleq\Pi_{\dagger_j}^2/\sum_{\dagger=1}^{z}\Pi_{\dagger_j}^2$, $\sum_{\dagger=1}^{z}\Pi_{\dagger_j}=\sum_{\dagger=1}^{z}\Lambda_{\dagger_j}=1$ *and* $\Pi_{\dagger_j}=1-\sum_{\nu=1;\nu\neq\dagger}^{z}\Pi_{\nu_j}$*, then in a similar proof approach, Theorem 1 will be valid provided that*

1. $\sigma_{k_{min}}\geq\frac{2\beta_k T_{k_{max}}\phi_{max}J_{k_{max}}^{(2)}}{\Pi_{k_{max}}}$
2. $\phi_{max}\leq\min_k\left\{\frac{\omega_k(B_{k_{min}}-\Omega_{k_{max}}-\Upsilon_k)}{\varepsilon N_{max}J_{k_{max}}\Xi_{k_{max}}(4d_{max}+\omega_k)}\right\}$

where $\Pi_{r_{max}}=1$, $\Pi_{l_{\dagger_{max}}}=\Pi_{\dagger_{max}}\triangleq\max_j\{\Pi_{\dagger_j}\}$, $\Xi_{r_{max}}\triangleq\max_j\{\Xi_{r_j}\}$, $T_{k_{max}}\triangleq\max_j\{T_{k_j}\}$ *and* $\Xi_{k_{max}\neq r_{max}}=1$.

Remark 2. *To determine admissible upper bound of the time-varying delays and the effects of the controller parameters on it, we need to find the upper bound using the conditions* (29) *and* (36) *whereby the system is stable. For the sake of simplicity, assume that* $\omega_k=1$*. Since* $\frac{2T_k}{\Pi_k}\leq 4d_{max}\Xi_k$*, by holding the following condition, the condition* (29) *will be held too.*

$$\sigma_{k_{min}}\geq 4d_{max}\Xi_k\beta_k\phi_{max}J_{k_{max}}^{(2)} \tag{38}$$

Therefore, to satisfy (38) *and given* (36)*, the following condition can be found for the upper bound of the time-varying delays.*

$$d_{max}\leq\min_k\left\{\frac{\varepsilon N_{max}\sigma_{k_{min}}}{4\left(\beta_k\Xi_k J_{k_{max}}^{(2)}\mathfrak{R}-\varepsilon N_{max}\sigma_{k_{min}}\right)}\right\} \tag{39}$$

where $\mathfrak{R}\triangleq\min_k\left\{\frac{B_{k_{min}}-\Omega_{k_{max}}-\Upsilon_k}{J_{k_{max}}\Xi_k}\right\}$*. The condition* (39) *implies that increasing* $\sigma_{k_{min}}$ *or* N_{max} *will improve the robustness of the system stability to the larger time delays. It is clear that increasing the parameter* N_{max} *expands the lower and upper bounds of the nonlinear function employed in the proposed controller.*

Next, we study the stability of the system (6) when the human operators exert nonpassive forces. Suppose that the remote robot is in contact with the environment which is assumed to be passive with respect to $\dot X_r$. Let the exerted forces be as

$$F_{e_k}=R_k-W_k\dot X_k,\qquad R_r=0 \tag{40}$$

where $R_{k\neq r}\in\mathbb{R}^{\varepsilon\times 1}$ is a positive bounded vector and $W_k\in\mathbb{R}^{\varepsilon\times\varepsilon}$ is a positive-definite diagonal matrix. Therefore, given (15), the closed-loop dynamics of the system can be rewritten as

$$M_k\dot\varphi_k+C_k\varphi_k=\Theta_k+J_k^T F_{e_k}+S_k(\Delta_k-\Sigma_k\varphi_k) \tag{41}$$

Theorem 2. *Consider the closed-loop dynamics* (41) *with the proposed controller* (7) *and the exerted forces* (40)*. Also, assume that the Jacobian matrices of the local manipulators are full rank and the time-varying delays are bounded. All signals in the system's state are bounded if*

1. $\sigma_{k_{min}}>\left(1+\frac{2\phi_{max}T_k}{\Pi_k}\right)\beta_k J_{k_{max}}^{(2)}$
2. $\phi_{max}\leq\min_k\left\{\frac{\omega_k(B_{k_{min}}-\Omega_{k_{max}}-\Upsilon_k)-\varepsilon N_{max}J_{k_{max}}}{\varepsilon N_{max}J_{k_{max}}\Xi_k(4d_{max}+\omega_k)}\right\}$

Proof. Given $V_2(x_t)$ (18) and $V_3(x_t)$ (19), let the Lyapunov-Krasovskii functional for the system be given as

$$V(x_t)=\sum_k\frac{1}{2}\Pi_k\varphi_k^T M_k\varphi_k+V_2(x_t)+V_3(x_t) \tag{42}$$

Adopting a similar approach used in the proof of Theorem 1 and given $\dot{X}_k^T P\left(\dot{X}_k\right) \leq \dot{X}_k^T \dot{X}_k \leq \beta_k J_{k_{max}}^{(2)} \varphi_k^T \varphi_k$, the time derivative of the functional (42) culminates in

$$\dot{V}(x_t) \leq \sum_k \Big(2T_k\phi_{max}\dot{X}_k^T P\left(\dot{X}_k\right) - \delta_k\sigma_{k_{min}}\varphi_k^T\varphi_k + \Pi_k\dot{X}_k^T R_k - \Pi_k\dot{X}_k^T W_k\dot{X}_k\Big) \leq \sum_{k\neq r}\left[(\Pi_k+2T_k\phi_{max})\beta_k J_{k_{max}}^{(2)} - \delta_k\sigma_{k_{min}}\right]\varphi_k^T\varphi_k + \sum_k \Pi_k R_k^T R_k + \left[2T_r\phi_{max}\beta_r J_{r_{max}}^{(2)} - \delta_r\sigma_{r_{min}}\right]\varphi_r^T\varphi_r \tag{43}$$

Therefore, the relationships

$$\begin{cases} \delta_k\sigma_{k_{min}} > (\Pi_k+2T_k\phi_{max})\beta_k J_{k_{max}}^{(2)} & if \quad k\neq r \\ \delta_k\sigma_{k_{min}} > 2T_k\phi_{max}\beta_k J_{k_{max}}^{(2)} & if \quad k=r \end{cases} \tag{44}$$

can be found as the sufficient conditions for

$$\dot{V}(x_t) < 0, \quad \forall \quad \|\varphi_r\| \geq \sqrt{\frac{\sum_k \Pi_k R_k^T R_k}{\delta_r\sigma_{r_{min}} - 2T_r\phi_{max}\beta_r J_{r_{max}}^{(2)}}} \tag{45}$$

Since $\Pi_k+2T_k\phi_{max} > 2T_k\phi_{max}$ and for the sake of simplicity, the following condition can be used to satisfy (44).

$$\delta_k\sigma_{k_{min}} > (\Pi_k+2T_k\phi_{max})\beta_k J_{k_{max}}^{(2)} \tag{46}$$

Now, we have to study the conditions under which the condition (46) is satisfied.

Case 1. $\left|\Delta_{k_i} - \sigma_{k_i}\varphi_{k_i}\right| \leq B_{k_i}$

It is clear that $\delta_k = \Pi_k$. Thus, given (46), the sufficient condition for (45) in this case would be

$$\sigma_{k_{min}} > \left(1 + \frac{2T_k\phi_{max}}{\Pi_k}\right)\beta_k J_{k_{max}}^{(2)} \tag{47}$$

Case 2. $|\Delta_{k_i} - \sigma_{k_i}\varphi_{k_i}| > B_{k_i}$

Since $\psi_k \leq \beta_k J_{k_{max}}^{(2)}$, by satisfying the following condition, the relation (34) is satisfied too.

$$\delta_k\sigma_{k_{min}} > \frac{\sigma_{k_{min}}\Pi_k\beta_k J_{k_{max}}^{(2)}\left(B_{k_{min}} - \Omega_{k_{max}} - \varepsilon\phi_{max}J_{k_{max}}\Xi_k N_{max} - \Upsilon_k\right)}{\varepsilon\sigma_{k_{max}}J_{k_{max}}N_{max}} \tag{48}$$

With respect to (48), the following condition should be held to satisfy (46).

$$\phi_{max} \leq \min_k \left\{ \frac{\omega_k\left(B_{k_{min}} - \Omega_{k_{max}} - \Upsilon_k\right) - \varepsilon N_{max}J_{k_{max}}}{\varepsilon N_{max}J_{k_{max}}\left(\frac{2T_k}{\Pi_k} + \omega_k\Xi_k\right)} \right\} \tag{49}$$

Now, since $\frac{2T_k}{\Pi_k} \leq 4d_{max}\Xi_k$, the following condition can be used to satisfy (49).

$$\phi_{max} \leq \min_k \left\{ \frac{\omega_k\left(B_{k_{min}} - \Omega_{k_{max}} - \Upsilon_k\right) - \varepsilon N_{max}J_{k_{max}}}{\varepsilon N_{max}J_{k_{max}}\Xi_k(4d_{max}+\omega_k)} \right\} \tag{50}$$

Upholding the conditions (47) and (50) guarantees (45) which in turn keeps all terms in $V(x_t)$ bounded. Thus, $\dot{X}_k, \varphi_k, e_k^0 \in L_\infty$ and noting (37) we get $e_k \in L_\infty$. Also, since $\dot{X}_k = J_k\dot{q}_k$ and $\dot{X}_k, \varphi_k \in L_\infty$, we get $\dot{q}_k, \zeta_r \in L_\infty$. Therefore, for large values of $\|\varphi_r\|$ the signals in the system's state are bounded, and so the proof of Theorem 2 completed. □

Remark 3. *In the case that the operators exert non-passive forces, we now study the force each operator percieves from the reflected force of the environment. Suppose that the remote robot is in a quasi-static hard contact with the environment, i.e., $\dot{q}_k, \ddot{q}_k \approx 0$ and is at a non-singular configuration. Given (5), we get $\varphi_l, \dot{\varphi}_l, \dot{\varphi}_r \to 0$ and using Property 5 we have $C_r\varphi_r \approx 0$. Also, regarding (50) and since*

$$\frac{\omega_k}{4d_{max}+\omega_k} < 1, \qquad \frac{1}{\Xi_k(4d_{max}+\omega_k)} > 0 \tag{51}$$

the condition (A.5) (see Appendix) is satisfied which guarantees that $|\Delta_k| \leq B_k$ and so $S_k(\Delta_k) = \Delta_k$. Therefore, considering the closed-loop dynamics (41) in the static hard contact scenario, we get

$$\begin{cases} F_{e_{l_\dagger}} - \Phi P_{l_\dagger}^0(.) \approx 0 \\ F_{e_r} - \mathfrak{I}^+\left[G_r - S_r\left(G_r - J_r^T\Phi P_r^0(.) + \Sigma_r\zeta_r\right)\right] \approx 0 \end{cases} \tag{52}$$

where $\mathfrak{I}^+$ is the pseudo-inverse of J_r^T. Consequently, the result in (52) implies that the position feedbacks provide the $\dagger^{th}$ operator with a preception of the reflected force from the environment equal to $\Phi P_{l_\dagger}^0(.)$. Therefore given (52), the error between an operator's perceived force and the environment's exerted force is guaranteed to be bounded.

Theorem 3. *Let the same conditions described in Theorem 1 still hold true. The task-space position errors (4) converge to the origin asymptotically in free motion ($\tau_{e_k} = 0$), regardless of whether $\Psi_r = 0$ or $\Psi_r \neq 0$.*

Proof. By integrating the both sides of (26) one can see that $\varphi_k \in L_2$. Based on the results of Theorem 1, $\varphi_k, \dot{X}_k, e_k \in L_\infty$. Also, considering Assumption 1 it can be concluded that $\dot{e}_k \in L_\infty$. Considering (5), $\varphi_k \in L_\infty$ and assuming that the redundant remote manipulator is able to avoid the singularities results in $\zeta_r \in L_\infty$ and so $\dot{q}_k \in L_\infty$ which in turn leads to $\dot{M}_k \in L_\infty$. Considering (1), since the term G_k is bounded, using Properties 1 and 5 of the system dynamics and given the boundedness of $S_k(\tau_k)$, it is possible to see that $\ddot{q}_k \in L_\infty$. Also, $\dot{q}_k, \ddot{q}_k \in L_\infty$ results in $\dot{\Psi}_r, \ddot{\Psi}_r \in L_\infty$. Furthermore, $\dot{q}_k, \ddot{q}_k, \dot{\Psi}_r, \ddot{\Psi}_r \in L_\infty$ and given the assumption that the redundant remote manipulator is able to avoid the singularities, $\dot{\zeta}_k, \ddot{\zeta}_k \in L_\infty$. Considering $\ddot{q}_k, \dot{\zeta}_k \in L_\infty$, it can be concluded that $\dot{\varphi}_k \in L_\infty$. Because $\varphi_k \in L_2$ and $\dot{\varphi}_k \in L_\infty$, using the Barbalat's lemma, $\varphi_k \to 0$. Considering (5), $\dot{q}_l \to 0$ and using the fact that $\dot{X}_k = J_k\varphi_k$, we get $\dot{X}_k \to 0$. If the redundant remote manipulator is able to avoid the singularities, then it can be obtained that $\dot{q}_r \to 0$. Applying $\tau_{e_k} = 0$ into (1) yields $\ddot{q}_k = M_k^{-1}\{-C_k\dot{q}_k - G_k + S_k(\Delta_k - \Sigma_k\varphi_k)\}$. Differentiating both sides with respect to time and given $\frac{d}{dt}\left(M_k^{-1}\right) =$

$-M_k^{-1}\left(C_k+C_k^T\right)M_k$, one can conclude readily that

$$\begin{aligned}\dddot{q}_k=&\frac{d}{dt}\left(M_k^{-1}\right)(-C_k\dot{q}_k-G_k+S_k(\Delta_k-\Sigma_k\varphi_k))\\&+M_k^{-1}\frac{d}{dt}(-C_k\dot{q}_k-G_k)-M_k^{-1}\dot{\Theta}_k\dot{S}_k(\Delta_k-\Sigma_k\varphi_k)\\&-M_k^{-1}\left(\frac{d}{dt}\left(J_k^T\Phi P_k(.)\right)+\Sigma_k\dot{\varphi}_k\right)\dot{S}_k(\Delta_k-\Sigma_k\varphi_k)\end{aligned}\quad(53)$$

On the basis of Properties 1 and 5, and given $\dot{q}_k\in L_\infty$, it is possible to see that $\frac{d}{dt}\left(M_k^{-1}\right)$ is bounded. Also, given

$$\begin{aligned}\frac{d}{dt}\left(J_k^T\Phi P_k(.)\right)=&\frac{d}{dt}\left(J_k^T\right)\Phi P_k(.)+J_k^T\Phi\frac{d}{dt}(P_k(.))=\frac{\partial}{\partial q_k}\left(J_k^T\right)\dot{q}_k\Phi P_k(.)\\&+\begin{cases}J_k^T\Phi\left(\Pi_\dagger\frac{\partial P(e_{\dagger r})}{\partial e_{\dagger r}}\dot{e}_{\dagger r}+\sum\limits_{\nu=1;\nu\neq\dagger}^{z}\Pi_\nu\frac{\partial P(e_{\dagger\nu})}{\partial e_{\dagger\nu}}\dot{e}_{\dagger\nu}\right) & \text{if}\quad k=l_\dagger\\ J_k^T\Phi\left(\sum\limits_{\dagger=1}^{z}\Pi_\dagger^2\frac{\partial P(e_{r\dagger})}{\partial e_{r\dagger}}\dot{e}_{r\dagger}\right) & \text{if}\quad k=r\end{cases}\end{aligned}\quad(54)$$

one can conclude that $\frac{d}{dt}(J_k^T\Phi P_k(.))\in L_\infty$. Now, let us investigate (53) in two cases as follows.

Case 1. $|\Delta_{k_i}-\sigma_{k_i}\varphi_{k_i}|\leq B_{k_i}$

Considering (2), it is possible to see that $\dot{s}_{k_i}(\Delta_{k_i}-\sigma_{k_i}\varphi_{k_i})=1$ *and given the facts that* $M_k^{-1}\dot{\Theta}_k=-\dot{\zeta}_k-M_k^{-1}\dot{M}_k\dot{\zeta}_k-M_k^{-1}\frac{d}{dt}(C_k\zeta_k+G_k)$, $\ddot{\zeta}_k,\dot{\varphi}_k\in L_\infty$ *and considering Properties 1, 3, 4 and 5, it is plausible to get* $\dddot{q}_k\in L_\infty$. *Given* $\dddot{q}_k\in L_\infty$ *and* $\ddot{\varphi}_k=\dddot{q}_k-\ddot{\zeta}_k$ *results in* $\ddot{\varphi}_k\in L_\infty$.

Case 2. $|\Delta_{k_i}-\sigma_{k_i}\varphi_{k_i}|>B_{k_i}$

Considering (2), it is easy to see that $\dot{s}_{k_i}(\Delta_{k_i}-\sigma_{k_i}\varphi_{k_i})=0$ *and from (53) it can be readily concluded that* $\dddot{q}_k\in L_\infty$. *Given* $\dddot{q}_k,\ddot{\zeta}_k\in L_\infty$ *results in* $\ddot{\varphi}_k\in L_\infty$.

Therefore, given $\ddot{\varphi}_k\in L_\infty$ and $\varphi_k\to 0$, and using the Barbalat's lemma we get $\dot{\varphi}_k\to 0$. Considering the closed-loop dynamics (15), noting (A.6) (see Appendix) and having shown that $\varphi_k,\dot{\varphi}_k\to 0$, we get $J_k^T\Phi P_k(.)\to 0$. Given $\dot{q}_k\to 0$ and $\dddot{q}_k\in L_\infty$, using the Barbalat's lemma results in $\ddot{q}_k\to 0$. Noting that in steady state ($\dot{q}_k=\ddot{q}_k=0$) $P_k(.)=P_k^0(.)$, we get $J_k^T\Phi P_k^0(.)\to 0$. Hence, if the redundant remote manipulator is able to avoid the singularities, then $P_k(.),P_k^0(.)\to 0$. Now assume that in (5) we have $\Psi_r=0$, then $\dot{q}_{l_\dagger},\ddot{q}_{l_\dagger}\to 0$ can still be concluded and we get $J_{l_\dagger}^T\Phi P_{l_\dagger}(.)\to 0$ and so $P_{l_\dagger}(.)\to 0$. Having $\dot{q}_{l_\dagger},\ddot{q}_{l_\dagger}\to 0$ and $P_{l_\dagger}(.)\to 0$, and regarding (8) one can readily conclude that $X_r(t-d_{r\dagger}(t))$ converges to a constant amount. Therefore, it is palatable to conclude that $P_{l_\dagger}^0(.)\to 0$. Reminding the property that for any $x_j\in\mathbb{R}$, $p_j(-x_j)=-p_j(x_j)$, we get $\sum_{\dagger=1}^{z}\Pi_\dagger P_{l_\dagger}^0(.)=\sum_{\dagger=1}^{z}\Pi_\dagger^2P(e_{\dagger r}^0)=-P_r^0(.)\to 0$ and so $P_r^0(.)\to 0$. Thus, we have $P_k^0(.)\to 0$ again. Simultaneously solving the equations of $P_k^0(.)\to 0$ and using the property that $p_j(x_j)$ passes through the origin, we get $e_k,e_k^0\to 0$. In other words, $e_k,e_k^0\to 0$ are valid for both $\Psi_r=0$ and $\Psi_r\neq 0$. Therefore, the proof of Theorem 3 has been completed. □

Remark 4. *Rearranging* $e_k^0\to 0$ *in matrix form we get*

$$\begin{bmatrix}\mathbb{I}_\varepsilon & -\mathbf{\Pi_2} & \dots & -\mathbf{\Pi_z} & -\mathbf{\Pi_1}\\ -\mathbf{\Pi_1} & \mathbb{I}_\varepsilon & \dots & -\mathbf{\Pi_z} & -\mathbf{\Pi_2}\\ \vdots & \vdots & \ddots & \vdots & \vdots\\ -\mathbf{\Pi_1} & -\mathbf{\Pi_2} & \dots & \mathbb{I}_\varepsilon & -\mathbf{\Pi_z}\\ -\mathbf{\Lambda_1} & -\mathbf{\Lambda_2} & \dots & -\mathbf{\Lambda_z} & \mathbb{I}_\varepsilon\end{bmatrix}\begin{bmatrix}X_{l_1}\\X_{l_2}\\ \vdots\\X_{l_z}\\X_r\end{bmatrix}\to\mathbf{0}_{\varepsilon(z+1)\times 1}\quad(55)$$

where $\mathbf{0}_{\varepsilon(z+1)\times 1}$ *denotes zero vector with dimension of* $\varepsilon(z+1)\times 1$, *and the notations* $\mathbf{\Pi}_\dagger$ *and* $\mathbf{\Lambda}_\dagger$ *stand for* $\Pi_\dagger\mathbb{I}_\varepsilon$ *and* $\Lambda_\dagger\mathbb{I}_\varepsilon$, *respectively. In the above equation, the matrix is not full rank and therefore there is a nonzero solution* $X_{l_1}=X_{l_2}=\dots=X_{l_z}=X_r$ *to the equation. Given (55) and with respect to the amount of the dominance factors, the following relationships can be deduced.*

$$\begin{cases}X_r,X_{l_{\nu\neq\dagger}}\to X_{l_\dagger} & if\quad \Pi_\dagger\to 1\\ X_{l_\dagger}\to\sum\limits_{\nu=1;\nu\neq\dagger}^{z}\Pi_\nu X_{l_\nu} & if\quad \Pi_\dagger\to 0\\ X_r\to\sum\limits_{\nu=1;\nu\neq\dagger}^{z}\Lambda_\nu X_{l_\nu} & if\quad \Pi_\dagger\to 0\end{cases}\quad(56)$$

The relations in (56) imply that an operator with the full dominance has a full control over all the robots, and the operator with the infinitesimal dominance has only an insignificant level of control over the remote robot, and its corresponding robot converges asymptotically to the weighted summation of the dominant robots' positions.

Remark 5. *From (55), it is obvious that* $\Lambda_\dagger$ *specifies the level of the authority of the* $\dagger^{th}$ *operator in controlling the remote robot. Therefore, how to adjust the operator's control power over the remote robot and the factors that affect it are especially important. To investigate this issue, let the dominance factor* $\Pi_\dagger$ *be assigned to the* $\dagger^{th}$ *local robot, and from the definition of the* $\Lambda_\dagger$, *one can rewrite it as*

$$\Lambda_\dagger=\frac{\Pi_\dagger^2}{\Pi_\dagger^2+\sum\limits_{\nu=1;\nu\neq\dagger}^{z}\Pi_\nu^2}=\frac{\Pi_\dagger^2}{\Pi_\dagger^2+\sum\limits_{\nu=1;\nu\neq\dagger}^{z}\left(\frac{a_\nu}{z-1}(1-\Pi_\dagger)\right)^2}\quad(57)$$

where $0\leq a_\nu\leq z-1$ *and* $\sum_{\nu=1;\nu\neq\dagger}^{z}a_\nu=z-1$. *Given the fact that* $\Pi_1+\dots+\Pi_z=1$, *from (57) we get*

$$\Lambda_\dagger=\frac{\Pi_\dagger^2}{\Pi_\dagger^2+(1-\Pi_\dagger)^2-2\sum\limits_{\nu=1;\nu\neq\dagger}^{z}\frac{a_\nu}{z-1}(1-\Pi_\dagger)\sum\limits_{\bar{\nu}=\nu+1;\bar{\nu}\neq\dagger}^{z}\frac{a_{\bar{\nu}}}{z-1}(1-\Pi_\dagger)}\quad(58)$$

where $\Lambda_\dagger$ *reaches its maximum amount when*

$$2\sum_{\nu=1;\nu\neq\dagger}^{z}\frac{a_\nu}{z-1}(1-\Pi_\dagger)\sum_{\bar{\nu}=\nu+1;\bar{\nu}\neq\dagger}^{z}\frac{a_{\bar{\nu}}}{z-1}(1-\Pi_\dagger)\quad(59)$$

takes up its maximum value, which can be shown readily that it occurs at $a_\nu=a_{\bar{\nu}}=1$ *or to be exact when the remaining local robots possess equivalent dominance-factors, i.e.,* $\Pi_\nu=\frac{1-\Pi_\dagger}{z-1}$, *in which z is the number of local robots. Therefore, from (58), the following relation can be found between the dominance-factor*

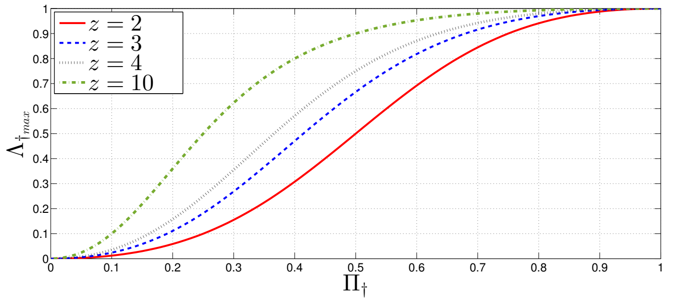

Figure 3: The relation between the number of local robots and the dominance factor of the $\dagger^{th}$ local robot.

$\Pi_\dagger$ and the consequent possible maximum authority ($\Lambda_{\dagger_{max}}$) of the $\dagger^{th}$ operator.

$$\Lambda_{\dagger_{max}}=\frac{\Pi_\dagger^2}{\Pi_\dagger^2+\frac{1}{z-1}(1-\Pi_\dagger)^2} \tag{60}$$

For different numbers of the local robots, the results for (60) are depicted in Figure 3. As it can be inferred from, by the increase in the number of local robots, a given dominance-factor would offer more control over the remote robot to the operator. In other words, when the number of local robots is higher, by a smaller dominance-factor, the operator can have an equivalent or higher level of authority in comparison to the case that the number of the local robots is smaller. For the sake of further clarity, Table 1 shows $\Lambda_{\dagger_{max}}$ for different values of dominance-factors when regarding the number of local robots.

Table 1: $\Lambda_{\dagger_{max}}$.

	z=2	z=3	z=4	z=10
$\Pi_\dagger$=0.1	0.01219	0.02410	0.03571	0.1000
$\Pi_\dagger$=0.5	0.50000	0.66667	0.75000	0.90000
$\Pi_\dagger$=0.9	0.98780	0.99387	0.99590	0.99863

Remark 6. *Suppose that the operators exert passive forces on the end-effectors of the local robots and the redundant remote manipulator is able to avoid the singularities. Also, assume that there is a passive contact force (F_{e_r}) between the remote robot's end-effector and the environment. Hence, $\varphi_k,\dot{\varphi}_k\to 0$ can still be concluded. Given $\phi_j p_{k_j}(.)\le\phi_{max}N_{max}$, and assuming that $F_{e_{l_{\dagger_j}}}\le\phi_j N_j$, we get*

$$\begin{cases} F_{e_{l_\dagger}}-\Phi P^0_{l_\dagger}(.)\to 0\\ F_{e_r}-\Phi P^0_r(.)\to 0\end{cases} \tag{61}$$

Considering (21), and given $p_j(-x_j)=-p_j(x_j)$ we get

$$P^0_r(.)=\sum_{\dagger=1}^{z}\Pi_\dagger\left(-P^0_{l_\dagger}(.)+\sum_{\nu=1;\nu\neq\dagger}^{z}\Pi_\nu P(X_{l_\dagger}(t)-X_{l_\nu}(t))\right)=\sum_{\dagger=1}^{z}-\Pi_\dagger P^0_{l_\dagger}(.) \tag{62}$$

Using (62), it can be concluded from (61) that

$$F_{e_r}+\sum_{\dagger=1}^{z}\Pi_\dagger F_{e_{l_\dagger}}\to 0, \tag{63}$$

from which one can infer that the reflected force from the environment is equal to the weighted summation of the forces perceived by the operators. Also, let us study the relation between the reflected force from the environment and the perceived forces with respect to the dominance factor. Given (61), we get

$$\begin{cases} F_{e_{l_\dagger}}+F_{e_r}\to 0 & if \quad \Pi_\dagger\to 1\\ F_{e_{l_\dagger}}+\left(\frac{\sum_{\nu=1;\nu\neq\dagger}^{z}\Pi_\nu P\left(e^0_{\nu\dagger}\right)}{\sum_{\nu=1;\nu\neq\dagger}^{z}\Pi_\nu^2 P\left(e^0_{r\nu}\right)}\right)F_{e_r}\to 0 & if \quad \Pi_\dagger\to 0\end{cases} \tag{64}$$

The relation (63) conveys the meaning that the operators' impact on the task can be adjusted by the dominance factors, and the formula in (64) clearly indicates that each operator has a level of perception of the reflected force according to his/her level of dominance over the task. For instance, when $\Pi_\dagger\to 1$, the $\dagger^{th}$ operator who has the full dominance over the task will perceive approximately the whole force reflected from the environment. Also, in the case that $\Pi_\dagger\to 0$, the system will project a fraction of the reflected force to the operator despite that its level of influence on the task is minute.

If $F_{e_{l_{\dagger_j}}}>\phi_j N_j$, then we get $F_{e_r}\to\Phi P^0_r(.)=-\sum_{\dagger=1}^{z}\Pi_\dagger\Phi P^0_{l_\dagger}(.)$. Also, $\sum_{\dagger=1}^{z}\Pi_\dagger^2 P(e^0_{r\dagger})\to 0$ is valid when the remote robot is in free motion.

Remark 7. *Given (52) and (61), for both the passive and non-passive cases, we have the relation*

$$F_{e_{l_\dagger}}-\Phi P^0_{l_\dagger}(.)\approx 0, \tag{65}$$

exploring which one can infer that the force each operator perceives is affected by the movement of all robots. However, the effect of robots owning bigger dominance-factors outweighs the ones possessing smaller dominance-factors. Also, one can readily infer that as $\Pi_\dagger\to 1$, the remote robot's movement predominantly determines the reflected force to the $\dagger^{th}$ operator. Also, when $\Pi_\dagger\to 0$, the reflected force to the $\dagger^{th}$ operator mainly depends on the movements of the remaining local robots, and the impact of the remote robot's movement on the reflected force pales into insignificance. These features make the proposed framework suitable for applications with training[1] processes.

Remark 8. *The mentioned properties make the proposed framework suitable for applications with training processes. However, we can modify the error signals and accordingly the control signals to tailor the Multi-Master/Single-Slave teleoperation especially to applications with literally cooperative purposes, in which the force each operator receives is affected only by the remote robot. To this end, consider the error signals modified as*

$$\begin{cases} e_{l_\dagger}\triangleq X_{l_\dagger}(t)-X_r(t-d_{r\dagger}(t))\\ e^0_{l_\dagger}\triangleq X_{l_\dagger}(t)-X_r(t)\\ e_r\triangleq X_r(t)-\sum_{\dagger=1}^{z}\Lambda_\dagger X_{l_\dagger}(t-d_{\dagger r}(t))\\ e^0_r\triangleq X_r(t)-\sum_{\dagger=1}^{z}\Lambda_\dagger X_{l_\dagger}(t),\end{cases} \tag{66}$$

[1] https://bit.ly/2WM2wiL

and the control signals (7) change accordingly, where

$$\begin{cases} P_{l_\dagger}(.) \triangleq \Pi_\dagger P(e_{\dagger r}); \quad e_{\dagger r} \triangleq X_{l_\dagger}(t) - X_r(t - d_{r\dagger}(t)) \\ P_r(.) \triangleq \sum_{\dagger=1}^{z} \Pi_\dagger^2 P\Big(X_r(t) - X_{l_\dagger}(t - d_{\dagger r}(t))\Big) \triangleq \sum_{\dagger=1}^{z} \Pi_\dagger^2 P(e_{r\dagger}) \end{cases} \tag{67}$$

The stability analysis of this controller is similar to the main controller's. Thus, we discuss only its outcomes related to the relation between the reflected forces, and the robots' desired positions. We have summed up the results as follows.

- *In steady state, and for the passive scenario:* $F_{e_r} + \sum_{\dagger=1}^{z} \Pi_\dagger F_{e_{l_\dagger}} \to 0$
- *In steady state, and for both the passive and nonpassive scenarios:* $F_{e_{l_\dagger}} \to \Phi P^0_{l_\dagger}(.)$
- *In steady state, and for the nonpassive scenario:* $F_{e_r} \approx \Im^+ \Big[G_r - S_r \Big(G_r - J_r^T \Phi P_r^0(.) + \Sigma_r \zeta_r \Big) \Big]$
- *In free motion:* $X_{l_\dagger}(t) = X_r$ *and* $X_r(t) = \sum_{\dagger=1}^{z} \Lambda_\dagger X_{l_\dagger}(t)$

such that $P_k^0(.)$ *stands for* $P_k(.)$ *in (67) when the time-delays are equal to zero. Please note that in the modified controller, the position exchange between the local robots is not required, and therefore, the local robots are not affected by the movement of their counterparts. This framework is not suitable for training since an operator with zero dominance will feel nothing, whether from the local robots' side or the remote robot's side. Also, the desired position for the remote robot is the weighted summation of local robots' positions. These properties make the modified controller suitable for cooperative[2] manipulation of the remote robot. Therefore, the rationale behind defining the error signals, in the form of (4) or (66), actually stems from the objectives we are tending to achieve.*

Remark 9. *Exploring the stability conditions of Theorem 1, for instance, in which the parameters* $J^{(2)}_{k_{max}}$*,* $\Omega_{k_{max}}$ *and* $J_{k_{max}}$ *are function of the robots' physical parameters, would provide clues as to how disparities between real (let be denoted by an overbar notation) and nominal values affect the system's stability. To analyze this effect and for the sake of simplicity, we assume that the sub-task control is not required. Thus, the stability conditions become*

1. $\sigma_{k_{min}} \geq \frac{2\beta_k T_k \phi_{max} J^{(2)}_{k_{max}}}{\Pi_k}$
2. $\phi_{max} \leq \min_k \left\{ \frac{\omega_k (B_{k_{min}} - \Omega_{k_{max}})}{\varepsilon N_{max} J_{k_{max}} \Xi_k (4d_{max} + \omega_k)} \right\}$

through which we study the effect of disparity in two cases as follows.

Nominal values are bigger than real values: *This leads to relations* $J^{(2)}_{k_{max}} > \bar{J}^{(2)}_{k_{max}}$*,* $\Omega_{k_{max}} > \bar{\Omega}_{k_{max}}$ *and* $J_{k_{max}} > \bar{J}_{k_{max}}$ *which consequently results in*

1. $\sigma_{k_{min}} \geq \frac{2\beta_k T_k \phi_{max} J^{(2)}_{k_{max}}}{\Pi_k} > \frac{2\beta_k T_k \phi_{max} \bar{J}^{(2)}_{k_{max}}}{\Pi_k}$
2. $\phi_{max} \leq \min_k \left\{ \frac{\omega_k (B_{k_{min}} - \Omega_{k_{max}})}{\varepsilon N_{max} J_{k_{max}} \Xi_k (4d_{max} + \omega_k)} \right\} < \min_k \left\{ \frac{\omega_k (B_{k_{min}} - \bar{\Omega}_{k_{max}})}{\varepsilon N_{max} \bar{J}_{k_{max}} \Xi_k (4d_{max} + \omega_k)} \right\}$

Therefore, using the nominal values, the system would be still stable.

Nominal values are lesser than real values: *This leads to relations* $J^{(2)}_{k_{max}} < \bar{J}^{(2)}_{k_{max}}$*,* $\Omega_{k_{max}} < \bar{\Omega}_{k_{max}}$ *and* $J_{k_{max}} < \bar{J}_{k_{max}}$ *which consequently results in*

1. $\sigma_{k_{min}} \geq \frac{2\beta_k T_k \phi_{max} J^{(2)}_{k_{max}}}{\Pi_k}$ *which does not satisfy* $\sigma_{k_{min}} \geq \frac{2\beta_k T_k \phi_{max} \bar{J}^{(2)}_{k_{max}}}{\Pi_k}$
2. $\phi_{max} \leq \min_k \left\{ \frac{\omega_k (B_{k_{min}} - \Omega_{k_{max}})}{\varepsilon N_{max} J_{k_{max}} \Xi_k (4d_{max} + \omega_k)} \right\}$ *which does not satisfy* $\phi_{max} \leq \min_k \left\{ \frac{\omega_k (B_{k_{min}} - \bar{\Omega}_{k_{max}})}{\varepsilon N_{max} \bar{J}_{k_{max}} \Xi_k (4d_{max} + \omega_k)} \right\}$

Therefore, using the nominal values, we should set the controller parameters far enough beyond the stability conditions' boundaries to keep the system stable.

Remark 10. *Given (36), when* $\varphi_k, \dot{\varphi}_k \to 0$ *then the term* Υ_k *is also converged to zero. Thus, let us define* $\phi_{k_{diss}} \triangleq \frac{\omega \Upsilon_k}{\varepsilon J_{k_{max}} N_{max} \Xi_k (4d_{max} + \omega)}$ *in which the subscript diss stands for the dissipation of the term* Υ_k*. Also, let* $\phi_{k_{fixed}} \triangleq \frac{\omega (B_{k_{min}} - \Omega_{k_{max}})}{\varepsilon J_{k_{max}} N_{max} \Xi_k (4d_{max} + \omega)}$ *be the parameter which is fixed throughout the control process. In other words, the condition (36) can be interpreted as* $\phi_{max} \leq \min_k \left\{ \phi_{k_{fixed}} - \phi_{k_{diss}} \right\}$*.*

4. Sub-task control for the remote robot

As mentioned earlier, the link velocity in the null space of J_r does not influence the task-space motion and does not contribute to the task-space velocity. Therefore, if it is such that tracks $(\mathbb{I}_m - J_r^+ J_r)\Psi_r$, then the movement of the telemanipulator in this configuration-dependent subspace can be regulated by Ψ_r. This kind of motion is called self-motion since it is not observed at the end-effector [59]. The function $[\mathbb{I}_m - J_r^+ J_r]\Psi_r$ can be considered as the desired velocity in the null space of J_r through which one can define an appropriate function for Ψ_r to complete the sub-task control. On the one hand, the sub-task tracking error for the redundant robot (let it be e_{ste}) was defined as $e_{ste} \triangleq [\mathbb{I}_m - J_r^+ J_r](\dot{q}_r - \Psi_r)$ [59] where, on the other hand, it can be shown as well as

$$e_{ste} \triangleq [\mathbb{I}_m - J_r^+ J_r](\dot{q}_r - \Psi_r) = [\mathbb{I}_m - J_r^+ J_r]\varphi_r \tag{68}$$

in which the property $[\mathbb{I}_m - J_r^+ J_r][\mathbb{I}_m - J_r^+ J_r] = \mathbb{I}_m - J_r^+ J_r$ has been used. Therefore, if $\varphi_r \to 0$ (Theorem 3), then the sub-task tracking error approaches the origin and the link velocity in the null space of J_r tracks $(\mathbb{I}_m - J_r^+ J_r)\Psi_r$. The gradient projection method [60] is utilized in this paper to achieve the sub-task control. As described in [32], the sub-task of the remote robot can be controlled by any differentiable auxiliary function Ψ_r provided that it is expressed in terms of the joint angles or the end-effector position. Hence, one can define a differentiable function $f(q_r)$: $\mathbb{R}^{m\times1} \to \mathbb{R}$ for which a lower value corresponds to more desirable configurations. Then, the auxiliary function $\Psi_r = -\frac{\partial}{\partial q_r} f(q_r)$ can be utilized for achieving the sub-task control of the remote robot.

[2] https://bit.ly/2WeDJ2w

5. Simulation and experiment results

In this section, the simulation and experimental results are presented as a vindication of the theoretical findings. For the sake of simplicity, we narrow down our study to a trilateral teleoperation system in which two human operators control the task-space position of a redundant remote manipulator through two local manipulators. To show the effect of the dominance factor in a comprehensible way, in the conduct of both the simulations and experiments, it is assumed that the operators exert their forces separately with an ample time interval in between. Before proceeding please note that you can find simulation and experimental videos associated with the following results in the footnotes.

5.1. Simulation results

The two local robots and the remote manipulator are considered to be 2-DoF and 3-DoF planar revolute-joint robots, respectively. The parameters $g{=}9.81m/s^2$, $m_{1_i}{=}m_{2_i}{=}0.4kg$, $m_{1_r}{=}m_{2_r}{=}m_{3_r}{=}0.35kg$, $L_{1_i}{=}L_{2_i}{=}0.45m$, $L_{1_r}{=}L_{2_r}{=}0.4m$, $\Omega_{i_{max}}{=}5.297$ and $\Omega_{r_{max}}{=}8.24$ are chosen where the subscript $i{\in}\{l_1,l_2\}$ denote the first and second local robots. It is assumed that the control signals are subjected to actuators saturation at levels $+20N.m$ and $-20N.m$ (i.e., $B_{k_i}{=}B_{k_{min}}{=}20N.m$). The forward and backward time delays are considered to be identical and equal to $d_r(t){=}d_l(t){=}0.05{+}0.05\sin(t)$ (i.e., $d_{max}{=}0.1sec$). The nonlinear function $p_j(x_j){=}\tan^{-1}(x_j)$ has been chosen (i.e., $N_j{=}N_{max}{=}\frac{\pi}{2}$) to be used in the controllers. Furthermore, $\min_k\left\{\phi_{k_{fixed}}\right\}{=}2.264$ and the gains $\phi_1{=}\phi_2{=}\phi_{max}$ are set. Also, $\sigma_{l_1}{\geq}0.648\phi_{max}$, $\sigma_{l_2}{\geq}0.648\phi_{max}$, $\sigma_{r_1}{\geq}1.694\phi_{max}$, $\sigma_{r_2}{\geq}1.694\phi_{max}$ and $\sigma_{r_3}{\geq}1.694\phi_{max}$ are considered. Therefore, the controllers used in the simulations are as

$$\tau_{l_1}{=}G_{l_1}{-}J_{l_1}^T\begin{bmatrix}\phi_{max} & 0\\ 0 & \phi_{max}\end{bmatrix}\Big(\Pi_1\tan^{-1}(e_{1r}){+}\Pi_2\tan^{-1}(e_{12})\Big) -\begin{bmatrix}0.648\phi_{max} & 0\\ 0 & 0.648\phi_{max}\end{bmatrix}\dot{q}_{l_1} \tag{69}$$

$$\tau_{l_2}{=}G_{l_2}{-}J_{l_2}^T\begin{bmatrix}\phi_{max} & 0\\ 0 & \phi_{max}\end{bmatrix}\Big(\Pi_2\tan^{-1}(e_{2r}){+}\Pi_1\tan^{-1}(e_{21})\Big) -\begin{bmatrix}0.648\phi_{max} & 0\\ 0 & 0.648\phi_{max}\end{bmatrix}\dot{q}_{l_2} \tag{70}$$

$$\tau_r{=}{-}\Theta_r{-}J_r^T\begin{bmatrix}\phi_{max} & 0\\ 0 & \phi_{max}\end{bmatrix}\Big(\Pi_1^2\tan^{-1}(e_{r1}){+}\Pi_2^2\tan^{-1}(e_{r2})\Big) -\begin{bmatrix}1.694\phi_{max} & 0 & 0\\ 0 & 1.694\phi_{max} & 0\\ 0 & 0 & 1.694\phi_{max}\end{bmatrix}\varphi_r \tag{71}$$

Initial conditions are given as $q_{l_1}(0){=}[\frac{\pi}{3},\frac{\pi}{3}]^T$, $q_{l_2}(0){=}[\frac{2\pi}{3},\frac{\pi}{2}]^T$ and $q_r(0){=}[\frac{\pi}{6},\frac{\pi}{6},\frac{\pi}{6}]^T$ for the first local robot, the second local robot and the remote robot, respectively. Also, it is assumed that all robots at $t{=}0$ sec are at rest i.e., $\dot{q}_k(0){=}\ddot{q}_k(0){=}0$. Given the remote robot's control law, it is important to assign an appropriate function to Ψ_r for the purpose of singularity avoidance. To this end, a common method is to define a function $f(q_r)$ for which a lower value is associated with a more desirable configuration. Motivated by [55, 59], in the simulations $\Psi_r{\triangleq}{-}0.01(q_{1_r}{-}2q_{2_r}{+}q_{3_r})[1,{-}2,1]^T$ is chosen for the singularity avoidance. Note that the selected Ψ_r is the negative of the gradient of the cost function $f(q_r){=}0.005(q_{3_r}{-}2q_{2_r}{+}q_{1_r})^2$ and the control law will try to minimize the cost function. To show the effectiveness of the proposed controller, the simulations are carried out in two scenarios as follows.

5.1.1. Free motion

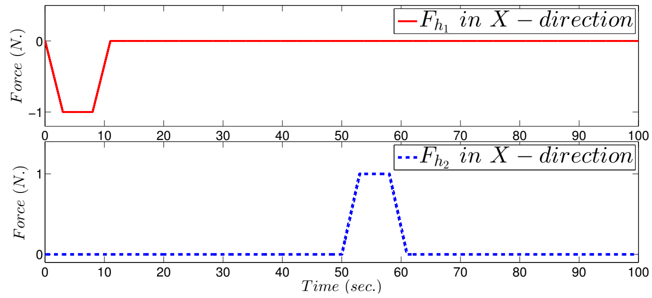

(a) The operators' applied forces

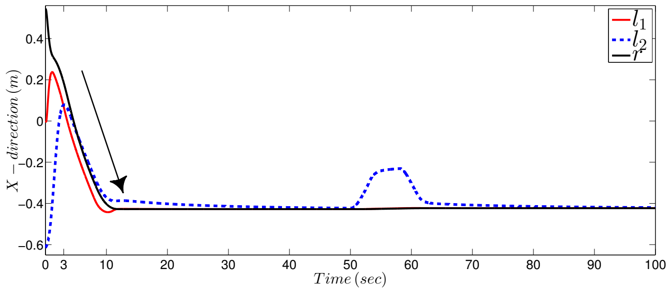

(b) $\Pi_1{=}0.99$ and $\Pi_2{=}0.01$

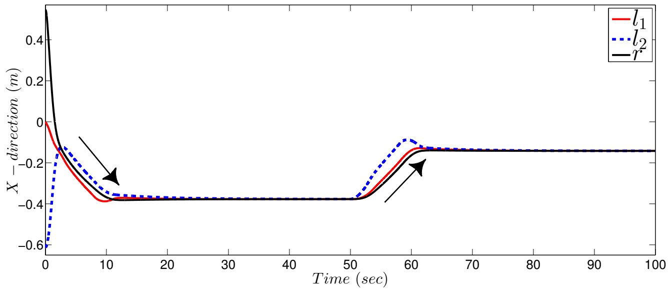

(c) $\Pi_1{=}0.5$ and $\Pi_2{=}0.5$

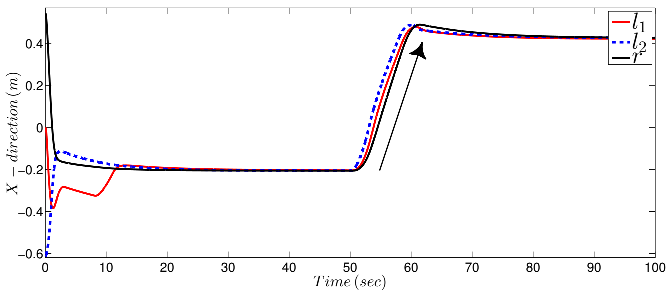

(d) $\Pi_1{=}0.01$ and $\Pi_2{=}0.99$

Figure 4: The operators applied forces and the positions of the end-effectors in $X{-}direction$ for the free motion scenario.

Suppose that the human operators apply their forces on the end-effectors of the local robots only in X-direction (for the sake of clarity in presentation) as shown in figure 4a where F_{h_1} denotes the first operator's applied force on the end-effector of the first local robot (l_1) and F_{h_2} denotes the second operator's applied force on the end-effector of the second local robot (l_2). Also, suppose that there is no obstacle in the remote site. Figure 4 shows the positions of the robots' end-effectors in X-direction for three different sets of the coefficients Π_1 and Π_2 used in the controllers (69)-(71). Now, let's elaborate on how these three sets affect the movement of the robots as follows.

Set 1. Π_1=0.99 *and* Π_2=0.01

The task-space positions using this set are shown in figure 4b. In terms of controlling the remote robot, the first human operator (first local robot) is superior to the second human operator (second local robot) due to its bigger dominance factor. The first operator has almost full control over the robots and therefore when exerts its force, the redundant remote robot's task-space position is forced to follow the first local robot's position. Also, the second local robot follows the first local robot because of its inferiority. On the other hand, when the second operator exerts its force, because it has insignificant dominance over the robots other than its own, the remote and first local robots do not follow the second local robot.

Set 2. Π_1=0.5 *and* Π_2=0.5

The task-space positions using this set are shown in figure 4c. In terms of controlling the remote robot, the first and second operators have equal dominance over the remote robot and on each other. Therefore, when they exert their forces, their corresponding robots are followed by the other robots but not as completely as when they have all but full control.

Set 3. Π_1=0.01 *and* Π_2=0.99

The task-space positions using this set are shown in figure 4d. In terms of controlling the remote robot, the second human operator is superior to the first human operator due to its bigger dominance factor. Therefore, when the second operator exerts its force, the redundant remote robot's task-space position is forced to follow the second local robot's position. Also, the first local robot follows the second local robot because of its inferiority. On the other hand, when the first operator exerts its force, because it has low dominance over the robots other than its own, the remote and second local robots do not follow the first local robot.

Note that as we see in figures 4b-4d and based on Remark 4 when the exerted forces subside to zero, the task-space positions converge to the same positions.

5.1.2. Contact motion

In this part, we study the contact motion of the robot in the remote site where there is assumed to be a stiff wall at X=−0.05 m. Suppose that the operators apply their forces on the end-effectors of the local robots as shown in figure 4a EXCEPT that the second operator applies in the opposite direction. It is also assumed that the wall behaves like a stiff spring with a stiffness of 10,000 N/m. Therefore, when the end-effector of the remote robot reaches the wall and tries to move further in negative X-direction, the feedback force in the positive X-direction will be F_{w_x}=−10000(X+0.05) N and in Y-direction will be F_{w_y}=0. Consequently, this reflected force inhibits the advance of the remote robot's end-effector through an equivalent torque of $J_r^T[F_{w_x}\,0]^T$ on the joints of the remote robot. Figure 5 shows the operators' applied forces, the wall's reflected force and the task-space positions of the robots in X-direction for three different sets of the coefficients Π_1 and Π_2. Given Remark 6, let's study these three sets as follows.

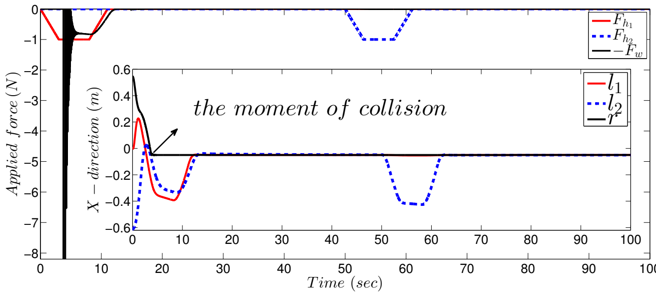

(a) Π_1=0.99 and Π_2=0.01

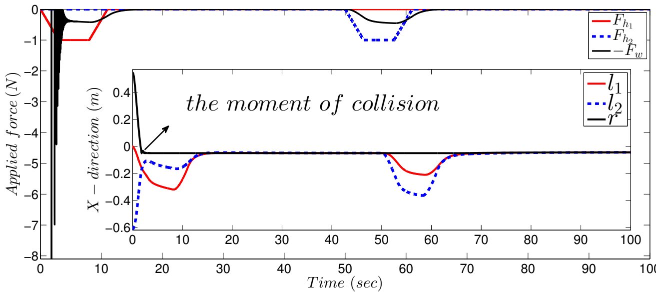

(b) Π_1=0.5 and Π_2=0.5

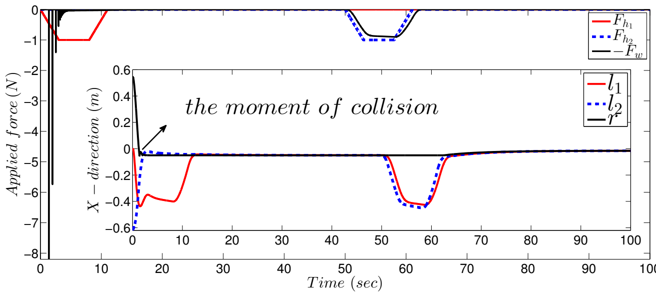

(c) Π_1=0.01 and Π_2=0.99

Figure 5: The exerted forces and the positions of end-effectors in X−*direction* for the contact motion scenario.

Set 1. Π_1=0.99 *and* Π_2=0.01

The task-space positions and the exerted forces using this set are shown in figure 5a. In this case, the first operator has virtually full control over the robots. Its applied force moves the first local robot and also makes the other robots to follow its task-space position in X-direction. Meanwhile, the remote robot collides with the wall and cannot move farther in negative X-direction. As the simulation indicates, the reflected force from the wall at first bursts ephemerally but then converges to the first operator's applied force ($-F_w \rightarrow 0.99F_{h_1}$). Also, when the second operator applies its force, its own robot moves but due to having practically no dominance over the other robots cannot make them follow the second local robot's task-space position in X-direction. The remote robot's end-effector is still in contact with the wall but due to the second operator's trivial dominance, the wall's reflected force pales into insignificance ($-F_w \rightarrow 0.01F_{h_2}$) when compared to the first operator's relevant reflected force.

Set 2. Π_1=0.5 *and* Π_2=0.5

The task-space positions and the exerted forces using this set are shown in figure 5b. In this case, the first and second operators have equal dominance over the remote robot and on each other. Therefore, when the first operator exerts its force, its corresponding robot is followed by the other robots but not as good as when it has full dominance. When the remote robot's end-effector reaches the wall, it collides with and cannot move further. The reflected force spikes briefly but then partially follows the operator's applied force ($-F_w \rightarrow 0.5F_{h_1}$). As the second operator applies its force, the remote robot is still in contact with the wall and virtually stands still in X-direction. The first local robot partly follows the second local robot and the reflected force follows the applied force in half part ($-F_w \rightarrow 0.5F_{h_2}$).

Set 3. Π_1=0.01 *and* Π_2=0.99

The task-space positions and the exerted forces using this set are shown in figure 5c. In this case, the second operator has almost full control over the robots and the first operator has virtually no dominance over the robots other than its own. The first operator's applied force moves the first local robot but cannot make the other robots to follow its task-space position in X-direction. Meanwhile, the remote robot collides with the wall and cannot move farther in negative X-direction. As the simulation indicates the reflected force initially surges but then cannot follow the first operator's applied force ($-F_w \rightarrow 0.01F_{h_1}$) and eventually dwindles to zero. Also, when the second operator applies its force, the remote robot is still in contact with the wall and practically cannot advance in the X-direction. Therefore, since the second operator has practically absolute dominance, the second local robot moves and makes the other local robot to follow its task-space position in X-direction. Also, the wall's reflected force tracks all but the second operator's applied force ($-F_w \rightarrow 0.99F_{h_2}$).

Note that as we see in figures 5a-5c and based on Remark 4 when the exerted forces subside to zero, the task-space positions converge to the same positions. The readers are encouraged to download and watch videos provided to help shed more light on the simulation results of the free motion[3] and contact motion[4] scenarios. Please note that since the applied forces in $Y-direction$ are zero, the synchronization error in $Y-direction$ is also slated to be zero in free motion.

5.2. *Experiment results*

To show the performance of the proposed controller in practice, we have experimented it on a trilateral teleoperation setup in which two local robots are connected to a remote robot.

Figure 6 shows the robots we have used to lay out the system. The 2-DoF first local robot is the upper-limb of rehabilitation robot 2.0 (Quanser Inc., Markham, ON, Canada) which has comparatively larger links and range of motion than the rehabilitation robot 1.0. The second local robot is a 2-DoF PHANToM 1.5A (Geomagic Inc., Morrisville, NC, USA) where the base joint of the 3-DoF PHANToM robot has been removed to transform it into a 2-DoF planar robot. The remote robot has four degrees of freedom and the 4-DoF planar RHI is developed by serially connecting two robots, a 2-DoF PHANToM 1.5A (Geomagic Inc., Morrisville, NC, USA) and a 2-DoF planar upper-limb rehabilitation robot 1.0 (Quanser Inc., Markham, ON, Canada). The base joint of the 3-DoF PHANToM robot has been detached to turn it into a 2-DoF planar robot. Also, to measure the applied forces on the second local robot and the remote robot, 6-DoF force/torque (f/t) sensors (50M31A3-I25, JR3 Inc., Woodland, CA, USA) are used. Furthermore, for the first local robot, a 6-DoF ATI Gamma Net force/torque sensor (ATI Industrial Automation, Inc., Apex, North Carolina, USA) is used. The link lengths for the first local, the second local and the remote robots are [0.34,0.375] m, [0.21,0.181] m and [0.254,0.1405,0.21,0.252] m, respectively.

Figure 6: Robots used in the experiment.

Like the simulation section, the experiments are conducted for the three different sets of the coefficients Π_1 and Π_2 and in two scenarios; free motion and contact motion. The performance paradigm of the system is the same as explained in the simulation section. Therefore, let's have a brief review of the conducted experiments as follows.

5.2.1. **Free motion**

In this scenario, it is assumed that the operators apply their corresponding forces separately and only in $X-direction$. Also, it is assumed that there is not an obstacle in the remote site.

Figure 7 shows an above view shot of the setup prepared for this scenario. Figure 8 shows the positions of the robots' end-effectors in X-direction for three different sets of the coefficients Π_1 and Π_2.

In figure 8a, Π_1=0.99 and Π_2=0.01 so that the first operator is superior to the second operator and has almost full control over all the robots. Therefore, when the first operator exerts its force, the redundant remote robot and the second local robot follow the first local robot. On the other hand, when the second operator exerts its force because it has insignificant dominance over the robots other than its own, the remote robot and the first local robot do not follow the second local robot.

In figure 8b, Π_1=0.5 and Π_2=0.5 so that the first and sec-

[3] https://bit.ly/2F5pb1R
[4] https://bit.ly/2ztvuGu

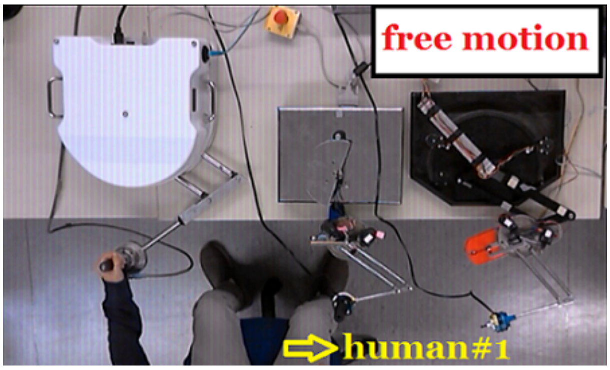

Figure 7: Trilateral teleoperation where the first and second local robots are manipulated by the human operators separately while the remote robot faces no obstacle in front of itself.

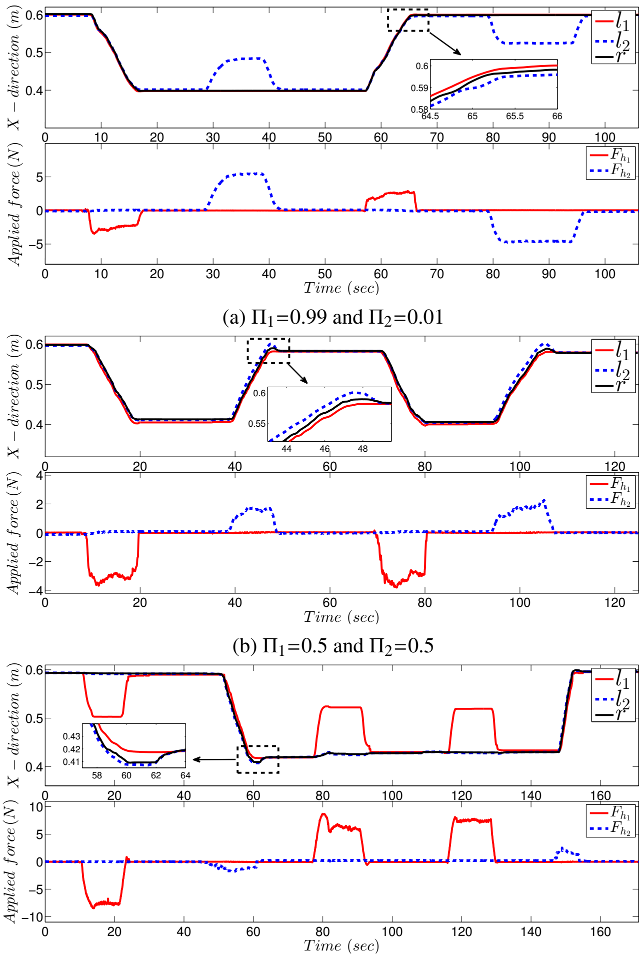

(a) Π_1=0.99 and Π_2=0.01

(b) Π_1=0.5 and Π_2=0.5

(c) Π_1=0.01 and Π_2=0.99

Figure 8: The experimental results of the exerted forces and the positions of the end-effectors in $X-direction$ for the free motion scenario.

ond operators have equal dominance over the remote robot and on each other. Thus, when they exert their forces, their corresponding robots are followed by the other robots but not as completely as when they have all but full control.

In figure 8c, Π_1=0.01 and Π_2=0.99 so that the second operator is superior to the first operator due to its bigger dominance factor. Therefore, when the second operator exerts its force, the redundant remote robot and the first local robot follow the second local robot. On the other hand, when the first operator exerts its force because it has trifling dominance over the robots other than its own, the remote robot and the second local robot do not follow the first local robot.

Note that as we see in figures 8a-8c and based on Remark 4, in the aftermath of the exerted forces' subsidence to zero, the task-space positions converge to the same positions.

5.2.2. Contact motion

In this scenario, it is assumed that the operators exert their corresponding forces separately and only in $X-direction$. Also, it is assumed that there is an obstacle in the remote site at x=0.5 m. Figure 9 shows an above view shot of the setup prepared for this scenario. Figure 10 shows the positions of the robots' end-effectors in X-direction for three different sets of the coefficients Π_1 and Π_2. Given Remark 6 let study these three sets as follows.

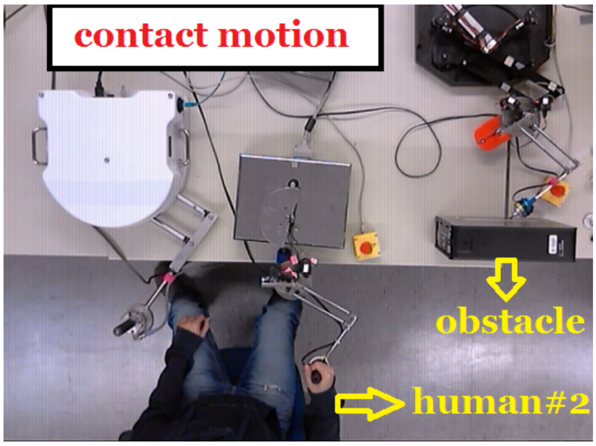

Figure 9: Trilateral teleoperation where the first and second local robots are manipulated by the human operators separately while the remote robot faces an obstacle in front of itself.

In figure 10a, Π_1=0.99 and Π_2=0.01 so that the first operator has virtually full control over the robots and its applied force not only moves the first local robot but also makes the other robots to follow its task-space position in X-direction. Meanwhile, the remote robot collides with the wall and cannot move farther in X-direction. The reflected force from the wall reaches a considerable proportion of the first operator's applied force. Also, the second operator's applied force moves its own local robot but due to its trivial dominance over the other robots cannot make them follow the second local robot's task-space position in X-direction and so the wall exerts almost nothing on the end-effector of the remote robot.

In figure 10b, Π_1=0.5 and Π_2=0.5 so that the first and second operators have equal dominance over the remote robot and on each other. Therefore, when the first operator exerts its force, its corresponding robot is followed by the other robots but not as good as when it has the full dominance. When the remote robot's end-effector reaches the wall, it collides with and cannot move farther. The reflected force partially follows the operator's applied force. As the second operator applies its force, the remote robot is still in contact with the wall and nearly stands

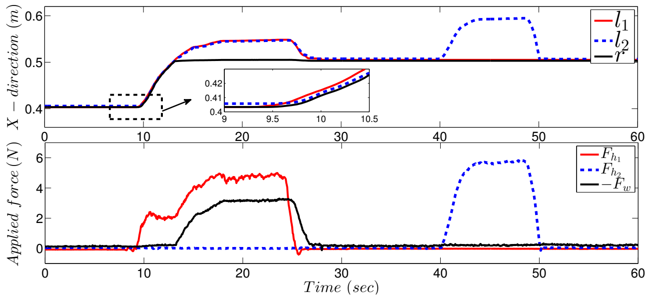

(a) Π_1=0.99 and Π_2=0.01

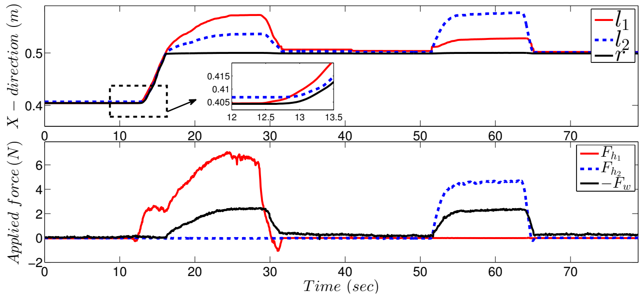

(b) Π_1=0.5 and Π_2=0.5

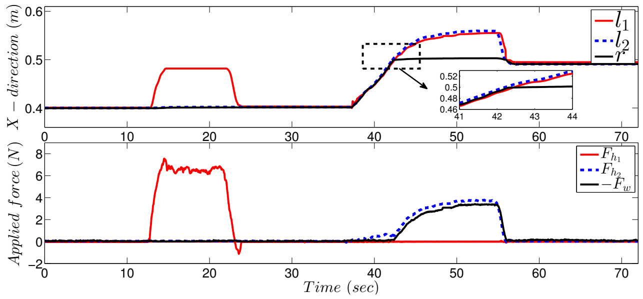

(c) Π_1=0.01 and Π_2=0.99

Figure 10: The experimental results of the exerted forces and the positions of the end-effectors in $X-direction$ for the contact motion scenario.

still in X-direction. The first local robot partly follows the second local robot and the reflected force reaches to practically a half proportion of the applied force.

In figure 10c, Π_1=0.01 and Π_2=0.99 so that the second operator has nearly full control over the robots and its applied force not only moves the second local robot but also makes the other robots to follow its task-space position in X-direction. Meanwhile, the remote robot collides with the wall and cannot move farther in X-direction. The wall exerts practically an equivalent amount of the second operator's applied force. Also, the first operator's applied force moves its own local robot but due to its trivial dominance over the other robots cannot make them follow the first local robot's task-space position in X-direction.

Note that as we see in figures 10a-10c and based on Remark 4, in the aftermath of the exerted forces' subsidence to zero, the task-space positions converge to the same positions. The readers are strongly encouraged to download and watch videos provided to help shed more light on the experimental results of the free motion[5] and contact motion[6] scenarios.

[5] https://bit.ly/2D7dEMQ

[6] https://bit.ly/2Qny48d

It is worth noting that given Remark 1 in case we have two local planar robots, settings $\Pi_{1_1}\simeq 1$, $\Pi_{1_2}\simeq 0$, $\Pi_{2_1}\simeq 0$, $\Pi_{2_2}\simeq 1$ such that $\Pi_{1_1}+\Pi_{2_1}=1$ and $\Pi_{1_2}+\Pi_{2_2}=1$ will enable the first local robot's operator to completely control the remote robot's end-effector in X-direction and the second local robot's operator to fully control the remote robot's end-effector in Y-direction.

6. Conclusion

In this paper, a novel control architecture was introduced for MM/SS teleoperation system, which enables several operators to control a redundant manipulator, cooperatively and based on their level of authority. For the MM/SS teleoperation, two series of error signals were defined, through each of which, the multilateral system can be geared up for either a training process or cooperative-based manipulation. The proposed controller satisfies the intended objectives in the presence of nonlinear dynamics, time-varying delays, and boundedness of the control signals. It was demonstrated that through the proposed framework, regardless of whether the operators apply passive or nonpassive forces, they can have a meaningful level of perception of the reflected force from the environment. Also, through the proposed framework, one can intentionally improve the system's tolerance to the bigger upper bound of time-varying delays. The asymptotic stability of the closed-loop dynamics was studied using a Lyapunov-Krasovskii functional under conditions on the controller parameters and the maximum values of time-varying delays. The efficiency of the proposed controller validated using numerical simulations with two 2-DoF planar local robots and a 3-DoF planar redundant remote robot. Also, to evaluate the performance of the proposed system in practice, experiments were done on a trilateral teleoperation system including two 2-DoF local planar robots, and one 4-DoF remote planar robot.

7. Appendix

Proof of lemma 1. *Equation (10) can be written as follows.*

$$\dot{X}_r^T\Phi\Big(P_r^0(.)-P_r(.)\Big)=\dot{X}_r^T\Phi\Bigg(\sum_{\dagger=1}^{z}\Pi_\dagger^2\Big(P\big(e_{r\dagger}^0\big)-P(e_{r\dagger})\Big)\Bigg)$$

$$=\sum_{j=1}^{\varepsilon}\dot{X}_{r_j}\phi_j\sum_{\dagger=1}^{z}\Pi_\dagger^2\Big(p_j\big(X_{r_j}-X_{l_{\dagger_j}}\big)-p_j\big(X_{r_j}-X_{l_{\dagger_j}}(t-d_{\dagger r})\big)\Big) \qquad \text{(A.1)}$$

$$\le\sum_{j=1}^{\varepsilon}\big|\dot{X}_{r_j}\big|\phi_j\sum_{\dagger=1}^{z}\Pi_\dagger^2\Big|p_j\big(X_{r_j}-X_{l_{\dagger_j}}\big)-p_j\big(X_{r_j}-X_{l_{\dagger_j}}(t-d_{\dagger r})\big)\Big|$$

Note that $X_{k_j},\dot{X}_{k_j}\in\mathbb{R}$ are the elements of $X_k,\dot{X}_k\in\mathbb{R}^{\varepsilon\times 1}$ vectors. Using the property that $|p_j(x_j)-p_j(y_j)|\le 2p_j(|x_j-y_j|)$ [24], inequality (A.1) can be written as

$$\le 2\sum_{j=1}^{\varepsilon}\big|\dot{X}_{r_j}\big|\phi_j\sum_{\dagger=1}^{z}\Pi_\dagger^2 p_j\Big(\Big|X_{l_{\dagger_j}}-X_{l_{\dagger_j}}(t-d_{\dagger r})\Big|\Big) \qquad \text{(A.2)}$$

Using $X_{l_{\dagger_j}} - X_{l_{\dagger_j}}(t-d_{\dagger r}) = \int_{t-d_{\dagger r}}^{t} \dot{X}_{l_{\dagger_j}}(\tau)d\tau$ *and* $|\int_{t-d_{\dagger r}}^{t} \dot{X}_{l_{\dagger_j}}(\tau)d\tau| \leq \int_{t-d_{\dagger r}}^{t} |\dot{X}_{l_{\dagger_j}}(\tau)|d\tau$*, inequality* (A.2) *can be written as*

$$\begin{aligned} &= 2\sum_{j=1}^{\varepsilon} |\dot{X}_{r_j}|\phi_j \sum_{\dagger=1}^{z} \Pi_\dagger^2 p_j\left(\left|\int_{t-d_{\dagger r}}^{t} \dot{X}_{l_{\dagger_j}}(\tau)d\tau\right|\right) \\ &\leq 2\sum_{j=1}^{\varepsilon} |\dot{X}_{r_j}|\phi_j \sum_{\dagger=1}^{z} \Pi_\dagger^2 p_j\left(\int_{t-d_{\dagger r}}^{t} \left|\dot{X}_{l_{\dagger_j}}(\tau)\right|d\tau\right) \end{aligned} \tag{A.3}$$

Using the inequality $p_j\left(\int_{t-d}^{t} |x_j(\tau)|d\tau\right) \leq \int_{t-d}^{t} p_j(|x_j(\tau)|)d\tau$ *[24], inequality* (A.3) *can be written as*

$$\begin{aligned} &\leq 2\sum_{j=1}^{\varepsilon} |\dot{X}_{r_j}|\phi_j \sum_{\dagger=1}^{z} \Pi_\dagger^2 \int_{t-d_{\dagger r}}^{t} p_j\left(|\dot{X}_{l_{\dagger_j}}(\tau)|\right)d\tau \\ &= 2|\dot{X}_r|^T \Phi \sum_{\dagger=1}^{z} \Pi_\dagger^2 \int_{t-d_{\dagger r}}^{t} P\left(|\dot{X}_{l_\dagger}(\tau)|\right)d\tau \\ &= 2\sum_{\dagger=1}^{z} \Pi_\dagger^2 |\dot{X}_r|^T \Phi \int_{t-d_{\dagger r}}^{t} P\left(|\dot{X}_{l_\dagger}(\tau)|\right)d\tau \end{aligned} \tag{A.4}$$

Therefore, the proof of inequality (10) *has been completed. The proof of the inequality* (11) *can also be concluded in a similiar way.*

Proof of inequality $\varphi_{k_i}(s_{k_i}(\Delta_{k_i} - \sigma_{k_i}\varphi_{k_i}) - \Delta_{k_i}) \leq 0$**.** *Following* (2)*, the second condition of Theorem 1 and the fact that* $\frac{\omega_k}{4d_{max}+\omega_k} \leq 1$*, we can conclude that*

$$\phi_{max} \leq \frac{B_{k_{min}} - \Omega_{k_{max}} - \Upsilon_k}{\varepsilon N_{max} J_{k_{max}} \Xi_k} \tag{A.5}$$

which results in (discernible from (A.9)*)*

$$\left|\Delta_{k_i}\right| \leq B_{k_i} \quad and \quad \Delta_{k_i} = s_{k_i}(\Delta_{k_i}) \tag{A.6}$$

Due to the strictly increasing property of the saturation function (2) *in the linear region*

$$\begin{cases} s_{k_i}(\Delta_{k_i} - \sigma_{k_i}\varphi_{k_i}) \leq s_{k_i}(\Delta_{k_i}) & if \quad \varphi_{k_i} \geq 0 \\ s_{k_i}(\Delta_{k_i} - \sigma_{k_i}\varphi_{k_i}) > s_{k_i}(\Delta_{k_i}) & if \quad \varphi_{k_i} < 0 \end{cases} \tag{A.7}$$

Therefore, it can be concluded that

$$\varphi_{k_i}(s_{k_i}(\Delta_{k_i} - \sigma_{k_i}\varphi_{k_i}) - \Delta_{k_i}) \leq 0 \tag{A.8}$$

and the proof of inequality has been completed.

Proof of inequality (31)**.**

$$\begin{aligned} &\left|-\theta_{k_i} - \sum_{j=1}^{\varepsilon} J_{k_{ji}}\phi_j p_{k_j}(.)\right| < \left|-\theta_{k_i}\right| + \left|\sum_{j=1}^{\varepsilon} J_{k_{ji}}\phi_j p_{k_j}(.)\right| \\ &< \Omega_{k_i} + \left|\sum_{\alpha=1}^{\beta_k}\left(M_{k_{i\alpha}}\ddot{\zeta}_{k_\alpha} + C_{k_{i\alpha}}\dot{\zeta}_{k_\alpha}\right)\right| + \phi_{max}J_{k_{max}} \sum_{j=1}^{\varepsilon} \Xi_k N_{max} \\ &< \Omega_{k_{max}} + \Upsilon_k + \varepsilon\phi_{max}J_{k_{max}}N_{max}\Xi_k \end{aligned} \tag{A.9}$$

References

[1] P. F. Hokayem, M. W. Spong, Bilateral teleoperation: An historical survey, Automatica 42 (12) (2006) 2035–2057.
[2] Y.-C. Liu, N. Chopra, Control of robotic manipulators under input/output communication delays: Theory and experiments, IEEE Transactions on Robotics 28 (3) (2012) 742–751.
[3] J.-P. Richard, Time-delay systems: an overview of some recent advances and open problems, automatica 39 (10) (2003) 1667–1694.
[4] R. J. Anderson, M. W. Spong, Bilateral control of teleoperators with time delay, IEEE Transactions on Automatic control 34 (5) (1989) 494–501.
[5] G. Niemeyer, J.-J. Slotine, Stable adaptive teleoperation, IEEE Journal of oceanic engineering 16 (1) (1991) 152–162.
[6] D. Lee, M. W. Spong, Passive bilateral teleoperation with constant time delay, IEEE transactions on robotics 22 (2) (2006) 269–281.
[7] N. Chopra, M. W. Spong, R. Lozano, Synchronization of bilateral teleoperators with time delay, Automatica 44 (8) (2008) 2142–2148.
[8] A. Forouzantabar, H. Talebi, A. Sedigh, Adaptive neural network control of bilateral teleoperation with constant time delay, Nonlinear Dynamics 67 (2) (2012) 1123–1134.
[9] H. Gao, T. Chen, H∞ estimation for uncertain systems with limited communication capacity, Automatic Control, IEEE Transactions on 52 (11) (2007) 2070–2084.
[10] H. Gao, T. Chen, J. Lam, A new delay system approach to network-based control, Automatica 44 (1) (2008) 39–52.
[11] E. Nuño, L. Basañez, R. Ortega, M. W. Spong, Position tracking for nonlinear teleoperators with variable time delay, The International Journal of Robotics Research 28 (7) (2009) 895–910.
[12] J.-H. Ryu, J. Artigas, C. Preusche, A passive bilateral control scheme for a teleoperator with time-varying communication delay, Mechatronics 20 (7) (2010) 812–823.
[13] Y. Kang, Z. Li, W. Shang, H. Xi, Motion synchronisation of bilateral teleoperation systems with mode-dependent time-varying communication delays, IET Control Theory & Applications 4 (10) (2010) 2129–2140.
[14] C.-C. Hua, X. P. Liu, Delay-dependent stability criteria of teleoperation systems with asymmetric time-varying delays, Robotics, IEEE Transactions on 26 (5) (2010) 925–932.
[15] I. Polushin, P. X. Liu, C.-H. Lung, Force reflection algorithm for improved transparency in bilateral teleoperation with communication delay, in: Robotics and Automation, 2006. ICRA 2006. Proceedings 2006 IEEE International Conference on, IEEE, 2006, pp. 2914–2920.
[16] R. Lozano, N. Chopra, M. W. Spong, Passivation of force reflecting bilateral teleoperators with time varying delay, in: Proceedings of the 8. Mechatronics Forum, 2002, pp. 954–962.
[17] C. Hua, X. P. Liu, Delay-dependent stability criteria of teleoperation systems with asymmetric time-varying delays, IEEE Transactions on Robotics 26 (5) (2010) 925–932. doi:10.1109/TRO.2010.2053736.
[18] D. Lee, M. W. Spong, Passive bilateral teleoperation with constant time delay, IEEE Transactions on Robotics 22 (2) (2006) 269–281. doi:10.1109/TRO.2005.862037.
[19] I. G. Polushin, P. X. Liu, C. Lung, Projection-based force reflection algorithm for stable bilateral teleoperation over networks, IEEE Transactions on Instrumentation and Measurement 57 (9) (2008) 1854–1865. doi:10.1109/TIM.2008.919874.
[20] M. V. Kothare, P. J. Campo, M. Morari, C. N. Nett, A unified framework for the study of anti-windup designs, Automatica 30 (12) (1994) 1869–1883.
[21] E. Arefinia, H. A. Talebi, A. Doustmohammadi, A robust adaptive model reference impedance control of a robotic manipulator with actuator saturation, IEEE Transactions on Systems, Man, and Cybernetics: Systems (2018) 1–12doi:10.1109/TSMC.2017.2759148.
[22] S.-J. Lee, H.-S. Ahn, Synchronization of bilateral teleoperation systems with input saturation, in: Control Automation and Systems (ICCAS), 2010 International Conference on, IEEE, 2010, pp. 1357–1361.
[23] S.-J. Lee, H.-S. Ahn, A study on bilateral teleoperation with input saturation and systems, in: Control, Automation and Systems (ICCAS), 2011 11th International Conference on, IEEE, 2011, pp. 161–166.
[24] F. Hashemzadeh, I. Hassanzadeh, M. Tavakoli, Teleoperation in the presence of varying time delays and sandwich linearity in actuators, Automatica 49 (9) (2013) 2813–2821.
[25] D.-H. Zhai, Y. Xia, Adaptive control for teleoperation system with vary-

ing time delays and input saturation constraints, IEEE Transactions on Industrial Electronics 63 (11) (2016) 6921–6929.
[26] J. Yan, Y. Wan, X. Luo, C. Chen, C. Hua, X. Guan, Formation control of teleoperating cyber-physical system with time delay and actuator saturation, IEEE Transactions on Control Systems Technology 26 (4) (2018) 1458–1467. doi:10.1109/TCST.2017.2709266.
[27] D. Zhai, Y. Xia, Finite-time control of teleoperation systems with input saturation and varying time delays, IEEE Transactions on Systems, Man, and Cybernetics: Systems 47 (7) (2017) 1522–1534. doi:10.1109/TSMC.2016.2631601.
[28] Y. Yang, J. Li, C. Hua, X. Guan, Adaptive synchronization control design for flexible telerobotics with actuator fault and input saturation, International Journal of Robust and Nonlinear Control 28 (3) (2018) 1016–1034.
[29] C. Hua, X. Yang, J. Yan, X. Guan, On exploring the domain of attraction for bilateral teleoperator subject to interval delay and saturated p + d control scheme, IEEE Transactions on Automatic Control 62 (6) (2017) 2923–2928. doi:10.1109/TAC.2016.2603780.
[30] N. Nath, E. Tatlicioglu, D. M. Dawson, Teleoperation with kinematically redundant robot manipulators with sub-task objectives, Robotica 27 (07) (2009) 1027–1038.
[31] P. Malysz, S. Sirouspour, A kinematic control framework for single-slave asymmetric teleoperation systems, Robotics, IEEE Transactions on 27 (5) (2011) 901–917.
[32] Y.-C. Liu, N. Chopra, Control of semi-autonomous teleoperation system with time delays, Automatica 49 (6) (2013) 1553–1565.
[33] Y.-C. Liu, Task-space bilateral teleoperation systems for heterogeneous robots with time-varying delays, Robotica 33 (10) (2015) 2065–2082.
[34] D.-H. Zhai, Y. Xia, Adaptive control of semi-autonomous teleoperation system with asymmetric time-varying delays and input uncertainties, IEEE transactions on cybernetics 47 (11) (2017) 3621–3633.
[35] M. Sharifi, H. Salarieh, S. Behzadipour, M. Tavakoli, Impedance control of non-linear multi-dof teleoperation systems with time delay: absolute stability, IET Control Theory & Applications 12 (12) (2018) 1722–1729.
[36] A. Zakerimanesh, F. Hashemzadeh, M. Tavakoli, Task-space synchronisation of nonlinear teleoperation with time-varying delays and actuator saturation, International Journal of Control 0 (0) (2018) 1–17. doi:10.1080/00207179.2018.1506158.
[37] D. Zhai, Y. Xia, A novel switching-based control framework for improved task performance in teleoperation system with asymmetric time-varying delays, IEEE Transactions on Cybernetics 48 (2) (2018) 625–638. doi:10.1109/TCYB.2017.2647830.
[38] M. Shahbazi, S. F. Atashzar, R. V. Patel, A systematic review of multilateral teleoperation systems, IEEE Transactions on Haptics 11 (3) (2018) 338–356. doi:10.1109/TOH.2018.2818134.
[39] Z. Li, C. Su, Neural-adaptive control of single-master–multiple-slaves teleoperation for coordinated multiple mobile manipulators with time-varying communication delays and input uncertainties, IEEE Transactions on Neural Networks and Learning Systems 24 (9) (2013) 1400–1413. doi:10.1109/TNNLS.2013.2258681.
[40] E. J. Rodriguez-Seda, J. J. Troy, C. A. Erignac, P. Murray, D. M. Stipanovic, M. W. Spong, Bilateral teleoperation of multiple mobile agents: Coordinated motion and collision avoidance, IEEE Transactions on Control Systems Technology 18 (4) (2010) 984–992. doi:10.1109/TCST.2009.2030176.
[41] X. Yang, C. Hua, J. Yan, X. Guan, Adaptive formation control of cooperative teleoperators with intermittent communications, IEEE Transactions on Cybernetics (2018) 1–10doi:10.1109/TCYB.2018.2826016.
[42] L. Zhang, J. Yan, X. Yang, X. Luo, F. Tan, X. Li, Consensus tracking for teleoperating cyber-physical system, International Journal of Control, Automation and Systems 16 (3) (2018) 1303–1311.
[43] J. Pliego-Jiménez, M. Arteaga-Pérez, Telemanipulation of cooperative robots: a case of study, International Journal of Control 91 (6) (2018) 1284–1299. arXiv:https://doi.org/10.1080/00207179.2017.1313455, doi:10.1080/00207179.2017.1313455.
URL https://doi.org/10.1080/00207179.2017.1313455
[44] D. Zhai, Y. Xia, Adaptive fuzzy control of multilateral asymmetric teleoperation for coordinated multiple mobile manipulators, IEEE Transactions on Fuzzy Systems 24 (1) (2016) 57–70. doi:10.1109/TFUZZ.2015.2426215.
[45] B. Khademian, K. Hashtrudi-Zaad, A framework for unconditional stability analysis of multimaster/multislave teleoperation systems, IEEE Transactions on Robotics 29 (3) (2013) 684–694. doi:10.1109/TRO.2013.2242377.
[46] P. Huang, P. Dai, Z. Lu, Z. Liu, Asymmetric wave variable compensation method in dual-master-dual-slave multilateral teleoperation system, Mechatronics 49 (2018) 1–10.
[47] S. Sirouspour, Modeling and control of cooperative teleoperation systems, IEEE Transactions on Robotics 21 (6) (2005) 1220–1225. doi:10.1109/TRO.2005.852254.
[48] Z. Lu, P. Huang, R. Cheng, Z. Liu, Z. Meng, Adaptive robust control for bimanual cooperative contact teleoperation with relative jacobian matrix, Journal of Intelligent & Robotic Systems (2018) 1–14.
[49] D. Sun, Q. Liao, X. Gu, C. Li, H. Ren, Multilateral teleoperation with new cooperative structure based on reconfigurable robots and type-2 fuzzy logic, IEEE Transactions on Cybernetics (2018) 1–15doi:10.1109/TCYB.2018.2828503.
[50] F. Hashemzadeh, M. Sharifi, M. Tavakoli, Nonlinear trilateral teleoperation stability analysis subjected to time-varying delays, Control Engineering Practice 56 (2016) 123–135.
[51] M. Sharifi, H. Salarieh, S. Behzadipour, M. Tavakoli, Stable nonlinear trilateral impedance control for dual-user haptic teleoperation systems with communication delays, Journal of Dynamic Systems, Measurement, and Control 139 (12) (2017) 121012.
[52] A. Zakerimanesh, F. Hashemzadeh, A. R. Ghiasi, Dual-user nonlinear teleoperation subjected to varying time delay and bounded inputs, ISA transactions 68 (2017) 33–47.
[53] Y. Ji, D. Liu, Y. Guo, Adaptive neural network based position tracking control for dual-master/single-slave teleoperation system under communication constant time delays, ISA transactions.
[54] M. Shahbazi, S. F. Atashzar, H. A. Talebi, R. V. Patel, Novel cooperative teleoperation framework: Multi-master/single-slave system, IEEE/ASME Transactions on Mechatronics 20 (4) (2015) 1668–1679.
[55] E. Zergeroglu, D. D. Dawson, I. W. Walker, P. Setlur, Nonlinear tracking control of kinematically redundant robot manipulators, IEEE/ASME Transactions on Mechatronics 9 (1) (2004) 129–132.
[56] M. W. Spong, S. Hutchinson, M. Vidyasagar, Robot modeling and control, Vol. 3, wiley New York, 2006.
[57] R. Kelly, V. S. Davila, J. A. L. Perez, Control of robot manipulators in joint space, Springer Science & Business Media, 2006.
[58] J. K. Hale, S. M. V. Lunel, Introduction to functional differential equations, Vol. 99, Springer Science & Business Media, 2013.
[59] P. Hsu, J. Mauser, S. Sastry, Dynamic control of redundant manipulators, Journal of Field Robotics 6 (2) (1989) 133–148.
[60] B. Siciliano, Kinematic control of redundant robot manipulators: A tutorial, Journal of Intelligent & Robotic Systems 3 (3) (1990) 201–212.